The Coso geothermal field: A nascent metamorphic core complex

F.C. Monastero[†]
A.M. Katzenstein
Geothermal Program Office, Naval Air Weapons Station, China Lake, California 93555-6108, USA

J.S. Miller
Department of Geology, San Jose State University, San Jose, California 95192-0102, USA

J.R. Unruh
William Lettis & Associates, Walnut Creek, California 94596, USA

M.C. Adams
Energy & Geosciences Institute, University of Utah, Salt Lake City, Utah 84108, USA

Keith Richards-Dinger
Geothermal Program Office, Naval Air Weapons Station, China Lake, California 93555-6108, USA

ABSTRACT

Investigation of the Coso Range using seismicity, gravity, and geochemistry of rocks and fluids, supports the interpretation that the structure hosting the geothermal resource is a nascent metamorphic core complex. The structural setting is a releasing bend in a dextral strike-slip system that extends from the Indian Wells Valley northward into the Owens Valley. This tectonic setting results in NW-directed transtension, which is accommodated by normal and strike-slip faulting of the brittle upper 4–6 km of the crust, and shearing and ductile stretching below this depth, accompanied by shallow igneous intrusions. Focal mechanisms of some small earthquakes that have occurred from 1996 to the present beneath the Coso Range exhibit depth-dependent rotation of seismic P and T axes, indicating that the local orientations of the principal stresses likely favor resolved shear stress on low-angle faults. These small earthquakes occur near the base of seismicity, which we interpret as coincident with the brittle-ductile transition. Geochemical results show a significant asthenospheric influence in the isotopic composition of rocks and fluids, indicating that the crust is thinned within the Coso structure. Thinned upper crust is underlain by a more dense mafic body at depths of 10 km or less. This is consistent with observed gravity anomalies and models. The mafic body may represent cumulates left over from the fractional crystallization of rhyolite, which occurs as endogenous domes at Coso, or it could be a sheeted-dike complex in the upper mid-crustal area. Transtension began at 2–3 Ma, and continues today. Using a long-term crustal deformation rate of 2 mm/yr, we infer that the basal detachment fault commonly observed in fully exhumed metamorphic core complexes will reach the surface in two to four million years.

Keywords: metamorphic core complex, brittle-ductile transition, geothermal, eastern California, transtension.

INTRODUCTION

Metamorphic core complexes were first recognized in the late 1970s through the work of Coney (1974), Crittenden et al. (1978), and Davis (1975, 1977). Their work built on earlier reconnaissance investigations of Misch (1960) and Armstrong (1968, 1972), who described the fundamental characteristics of metamorphic core complexes as low-angle normal faults that juxtapose disparately metamorphosed rocks above and below. The term metamorphic core complex was introduced by Crittenden et al. (1978) as a generic description of structures that occur widely in the western United States. Since 1978, there has been a proliferation of investigations on the nature, origin, and mechanisms of formation of metamorphic core complexes (for a summary, see Davis and Lister, 1988, and Beratan, 1996).

A typical metamorphic core complex is characterized by an extended upper plate of fault-bounded blocks resting structurally on a lower plate of highly metamorphosed rocks that have been subjected to ductile deformation (Fig. 1). The structural contact between the brittle upper-plate rocks and metamorphosed lower-plate rocks commonly is a mylonitic shear zone. Upper-plate faults are observed to terminate against, or sole into, this shear zone. Additional features of fully exhumed metamorphic core complexes suggest that certain conditions were operational during formation of the structures, including hydrothermal alteration related to coeval heating and possibly volcanism (Fig. 1), and pervasive faulting and fracturing from coeval tectonic activity. Exposure of the lower-plate rocks in a typical metamorphic core complex is attributed to uplift and doming in response to extreme attenuation of the upper plate, presumably in the latter stages of the evolution of the structure. The question this paper is concerned with, however, is what a very young, or "nascent," metamorphic core complex would look like prior to exhumation and exposure of the lower plate.

In this paper we show that the Coso geothermal area in eastern California has many of the features of an immature metamorphic core complex. We summarize the structural setting and salient features of exhumed metamorphic core complexes, and go on to describe the tectonic, structural, seismological, geophysical, and geochemical characteristics of the Coso Range that are consistent with the hypothesis that this region is an actively developing, but immature, metamorphic core complex. Finally, we will show that the location and geologic structure of
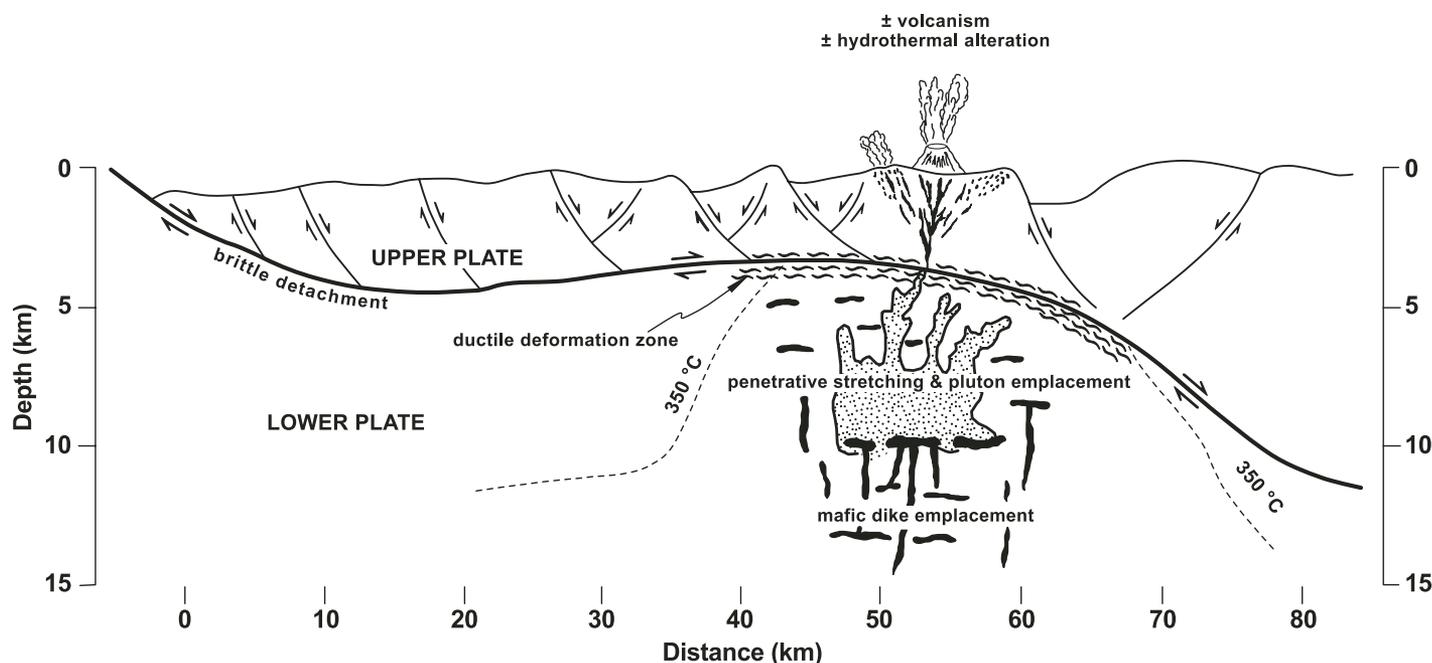
[†]E-mail: francis.monastero@navy.mil.

Figure 1. Diagram of common features of metamorphic core complexes in the middle stages of development, i.e., neither the basal mylonitized detachment zone nor the lower plate is exhumed. Faults are highly stylized, but accurately reflect the types that have been found in the upper plate (hanging wall) of fully exhumed metamorphic core complexes. Adapted from Gans et al. (1985), Lister et al. (1984), and Fournier (1999). Vertical exaggeration = 2×.

the area are the result of transtension associated with the Pacific–North America plate boundary.

Structural Setting and Characteristics of Metamorphic Core Complexes

In the southwestern United States, metamorphic core complexes are widely distributed in western Arizona, eastern California, and eastern Utah, and are among the most intensively studied tectonic features in the United States (see, for instance, Gans et al., 1985; Wust, 1986; Livaccari et al., 1995; Fletcher et al., 1995). They characteristically are found in regions that have undergone large amounts of Cenozoic crustal extension and thinning (e.g., the southern and northern Great Basin), and areas that have been subjected to transtension (e.g., Walker Lane and Death Valley). Examples of the former include the Central Mojave metamorphic core complex (Fletcher et al., 1995) and the Snake Range (Gans et al., 1985). Notable among the latter are the Funeral Mountains (Serpa and Pavlis, 1996), the Mineral Mountains (Glazner et al., 1994), and the Black Mountains (Holm et al., 1993). Although there are differences in the geometries of the faults that bound these structures, they all require thinning of the crust to accommodate extension in the horizontal plane.

Another common feature of metamorphic core complexes is the presence of magmatism.

Glazner and Ussler (1989) discussed the role of magmatism as it relates to regional extension in the southwestern United States and concluded that associated crustal thinning increases the average crustal density and promotes eruption of basalts. Lister and Baldwin (1993) contend that the formation of metamorphic core complexes may, in fact, be dependent on syntectonic mafic intrusions that heat the crust and facilitate formation of a brittle-ductile transition zone. Buck (1991) asserted that core complexes formed in areas of high heat flow with contemporaneous volcanism, consistent with Coney and Harms' (1984) observation that formation of metamorphic core complexes in what is now the southwestern United States was facilitated by a pulse of volcanism related to subduction of young, hot lithosphere as the Farallon plate spreading ridge approached North America. They proposed that this heated the crust and reduced the effective viscosity of the lithosphere, which then promoted wholesale crustal thinning. Christiansen (1989), Gans et al. (1985), Smith et al. (1990), Miller and Miller (1991), Davis and Hawkesworth (1993), and Walker et al. (1995) showed that calc-alkaline magmatism occurred prior to, or during, extensional events, which may have softened the crust and thereby enabled unroofing of the metamorphic core complexes. Parsons and Thompson (1993) argued that mid-crustal magmatism associated with metamorphic core

complex formation results in thermal softening of the crust, increased horizontal strain, and rotation of principal stress axes, thus facilitating formation of low-angle normal faults commonly found in the brittle upper plate (cf. Fig. 1) of fully exhumed metamorphic core complexes.

Examples of Youthful Metamorphic Core Complexes

Although the vast majority of well-studied core complexes are fully exhumed, there are examples reported in the literature of metamorphic core complexes that are in the formative stages. A brief examination of the characteristics of these will provide valuable clues to what is important in recognizing a nascent metamorphic core complex.

The Woodlark–D'Entrecasteaux extensional province in Papua New Guinea is such an example (Abers, 1991, and Hill et al., 1995); it is associated with a zone of high seismicity, is in close proximity to an active volcanic field, and is in an area of localized extension bounded by strike-slip faults. Hill et al. (1995) described syntectonic introduction of asthenospheric mantle material that produced temperature and pressure conditions conducive to: development of shallow silicic plutons and associated magmatism; formation of metamorphic rocks in the lower plate; and facilitation of stress conditions

for the occurrence of low-angle normal faults (Abers et al., 1997).

Another nonexhumed core complex has been postulated at Larderello, Italy, on the western coast of the province of Tuscany (Franceschini, 1995) in an area that has pervasive surface geothermal activity. Using reflection seismology, investigators have identified an antiformal reflector that they refer to as the "K" horizon, which lies at or near the local base of seismicity, coincides with a zone of intense metamorphism found in geothermal exploration wells, and is interpreted to be a ductile, mylonitic detachment fault (Franceschini, 1995). The "K" horizon has been penetrated by two wells, which encountered near-lithostatic fluid pressures and temperatures in excess of 400 °C (Cappetti et al., 1985). Fournier (1991, 1999) pointed out that fluids found in shallow hydrothermal systems that have temperatures near that necessary for the ductility of quartz-rich rocks (≥350 °C) have associated hydrostatic pore fluid pressures. These fluids generally occur at 3.5–5.0 km depth beneath the impermeable brittle-ductile transition (Fournier, 1999). In this type of environment, any fractures that form as a result of brittle failure due to transient strain rate perturbations will subsequently seal as a consequence of ductile flow, thus there will be no permeability, and the system will form an impermeable seal: the brittle-ductile transition (Fournier, 1999). Fluids beneath the brittle-ductile transition can attain lithostatic pressure equilibrium, whereas those above the transition are at hydrostatic pressure. The "K" horizon does not, however, crop out, so if the Larderello field is indeed a core complex and the "K" horizon is the brittle-ductile transition, then the metamorphic core complex must be in the formative stages.

LOCATION AND TECTONIC SETTING OF THE COSO FIELD

The Coso geothermal field is located in the Coso Range in east-central California (Fig. 2) within an area that Wernicke (1992) referred to as the southwest Basin and Range. Coso is situated east of the Sierra Nevada front in a zone of high seismicity that produced a magnitude 7.5 earthquake in 1872 (Beanland and Clark, 1994) and a magnitude 5.8 event in 1995 in the Indian Wells Valley. Both earthquakes were dextral strike-slip events, manifest of the long-lived transtensional domain that has been active in the southwestern Basin and Range for the past 16 m.y. (Wernicke et al., 1982; Hodges et al., 1989; Schweig, 1989; Bacon et al., 1982). The Sierra Nevada–Central Valley ("Sierran") microplate that forms the western margin of the southwest Basin and Range currently is moving

~12–14 mm/yr in a northwest direction relative to stable North America (Argus and Gordon, 2001; Dixon et al., 2000). Wernicke et al. (1982) presented evidence for 120 km of right-lateral transtensional displacement along the northern Death Valley fault zone, and 20–40 km of extension in Panamint, Saline, and Owens Valleys, all of which has accommodated large-scale translation of the Sierra Nevada with respect to the Colorado Plateau during late Cenozoic time. Monastero et al. (2002) described at least 10 km of additional westward-directed extension in the Indian Wells Valley during the latest Miocene(?) and Pliocene. Thus, the minimum total extension in the southwest Basin and Range is estimated at 150–170 km. Geodetic observations (McCluskey et al., 2001) indicate that up to half of the present Sierran–North American motion at the latitude of Coso is accommodated by distributed dextral shear (Oldow, 2003) along a series of poorly integrated strike-slip and normal faults in the Owens, Rose, and Indian Wells Valleys. The Coso geothermal area occurs within this zone in the middle of a releasing stepover between two dextral faults (Unruh et al., 2002a).

Early geological studies of the Coso Range recognized the youthful nature of the volcanic features found there (Schultz, 1937; Evernden et al., 1964), although a definitive study of the volcanic geology of Coso was not published until Duffield and Bacon (1981). One of the relevant geologic features of the Coso Range is the strongly bimodal Pleistocene (1.1–0.033 Ma) rhyolite-basalt rocks and associated tephra. Although small in volume, they attest to youthful volcanism associated with the site (Duffield, et al., 1980), as do the abundant hot springs, fumaroles, and mud pots.

Structural Setting of the Coso Range

Weaver and Hill (1979) were the first to suggest that seismicity within the Coso Range defined a releasing bend in a dextral strike-slip fault system. Roquemore (1981) also interpreted that active deformation in the Coso region reflects distributed crustal shear and strike-slip faulting. Analysis of seismicity data acquired over the past fifteen years confirms these observations, and places the principal boundary faults of the strike-slip system in the Indian Wells Valley on the southwest and the Wild Horse Mesa area on the northeast (Fig. 2). The dimensions of this stepover are ~100 km in length by 60 km in width. The Little Lake fault zone that defines the southwestern boundary of the Coso stepover (Fig. 2) dextrally offsets 465 ka basaltic lava flows (Roquemore, 1981). A swarm of events occurred in 1982 in the central Indian Wells Valley along the projected buried trace of the Little

Lake fault, highlighted by a M_L 5.2 event, the focal mechanism of which exhibited nearly pure dextral slip on a NW-striking nodal plane.

The northeastern boundary of the stepover is not as well defined, but probably is located between the edge of Wild Horse Mesa and Lower Centennial Flat (Fig. 2). Streitz and Stinson (1977) showed a buried NW-striking fault in the Lower Centennial Flat, but no sense of offset was indicated. Based on geophysical data and modeling, Pakiser et al. (1964) also concluded that a fault with this orientation projected north-northwestward from Lower Centennial Flat into Owens Lake. Over a 9 yr period (1991–2000) there were several earthquake swarms that occurred within the Coso Range that defined a NW-trending fault zone (Bhattacharyya et al., 1999), referred to herein as the Wild Horse Mesa fault (WHMF in Fig. 2). Based on detailed analysis of these swarms and their associated focal mechanisms, Unruh et al. (2002a) identified a blind, right-lateral strike-slip fault beneath eastern Wild Horse Mesa, which is a potential candidate for the eastern boundary of the stepover. The blind fault strikes northwest, suggesting that the locus of dextral shearing may pass through the northwestern Coso Range onto the Owens Valley fault in southwestern Owens Lake basin, rather than through the eastern to northeastern part of the Coso Range, as inferred by Pakiser et al. (1964) and Stinson (1977). Further field mapping is currently under way to better define this northeastern boundary.

The Airport Lake fault (Fig. 2) is a major dextral strike-slip structure that traverses the Indian Wells Valley and appears to terminate at the eastern end of the White Hills anticline. It is a seismogenic fault that supported three earthquakes in late 1995 and early 1996, ranging in magnitude from 5.2 to 5.8. Focal mechanisms and aftershock patterns for these events indicate that they occurred on a NNW-trending, dextral, strike-slip structure. As we will discuss below, the Airport Lake fault is analogous to a cross-basin fault that typically forms in analog models of stepover structures.

Global positioning system (GPS) data acquired annually from 1993 until 2000 in the Coso Range and surrounding areas (McCluskey et al., 2001) show that there is an average of 6.5 ± 0.7 mm/yr of dextral shearing across the Coso Range and the Indian Wells Valley (Fig. 3). Note that the authors assumed an elastic model with a locking depth of 15 km on major faults. Three E-NE–oriented velocity profiles (Fig. 4) drawn through the area reveal that the crustal velocity can be described as a continuous, 60-km-wide zone of deformation. However, within this zone there are apparent discrete 1.5–3.0 mm/yr steps that, in some instances (e.g., the Airport Lake
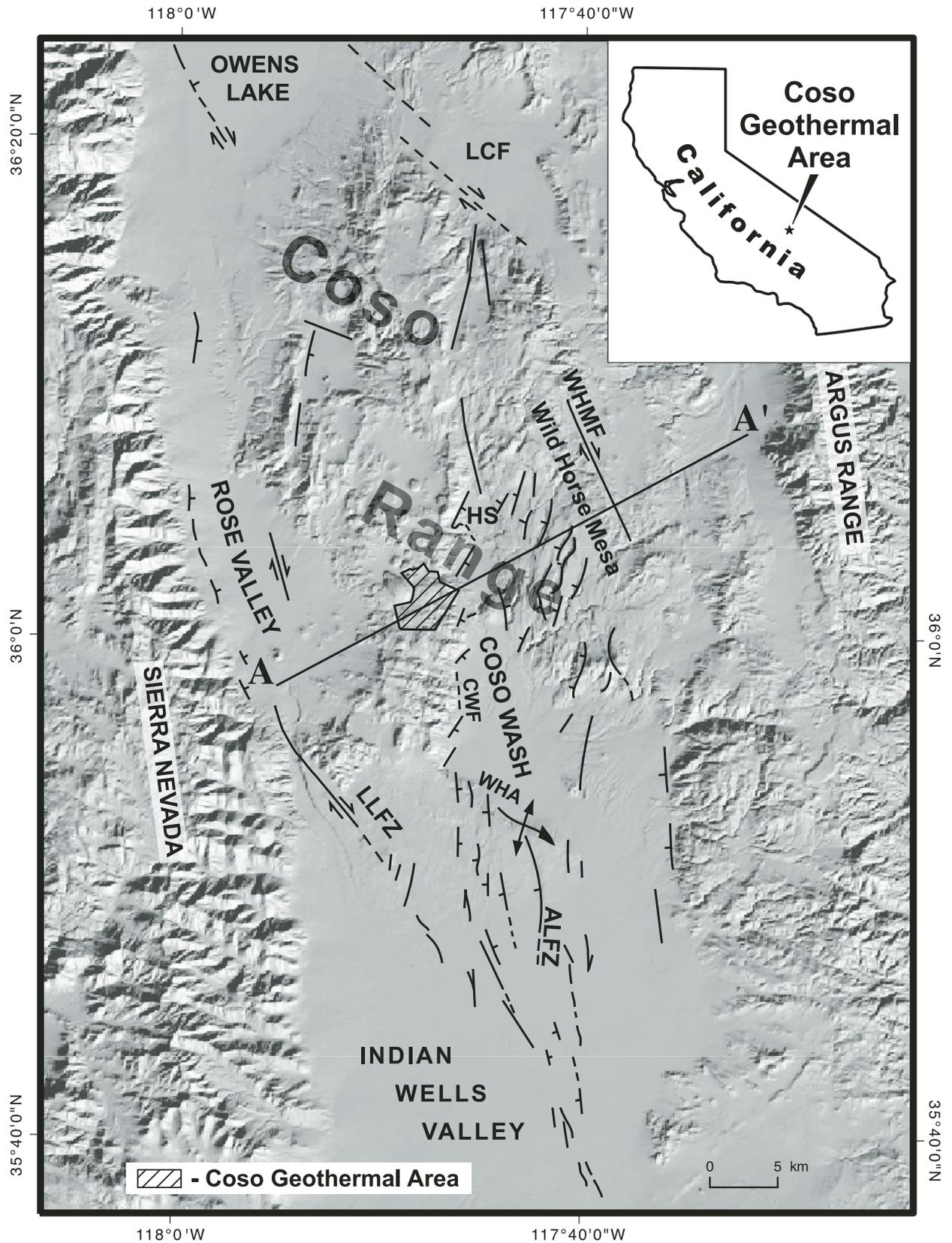
Figure 2. Location map and major geographic and geologic features discussed in this paper. Coso Range, Little Lake fault zone (LLFZ), Airport Lake fault zone (ALFZ), Coso Wash fault (CWF), White Hills anticline (WHA), Wild Horse Mesa fault (WHMF), Lower Centennial Flat (LCF), Haiwee Spring (HS). Faults are designated as heavy black lines, dashed where approximate. Arrows indicate sense of offset on faults, and tick mark is on downthrown block of normal faults.

fault zone and the Coso Wash fault zone), correspond to active fault zones. In other instances, such as between BM 25 and FORK on profile A, the 2 mm/yr step is not associated with a known, active fault, although the area has experienced several earthquake swarms over the past 15 yr. Within the limits imposed by the GPS sampling locations, these discrete steps correspond to the locations of the major faults in the Coso stepover, attesting to the dynamic character of that structure.

Analog Modeling of Releasing Bend Configurations

Analog modeling provides insights into the evolution of pull-apart basins and provides a ready comparison for structures found in the Coso stepover (Dooley and McClay, 1997; Rahe et al., 1998; Sims et al., 1999). Basin boundaries, symmetry, and internal structures in the models vary according to whether the substrate was ductile or nonductile, the rate of displacement of opposite sides of the strike-slip system, and the obliquity of the angle of displacement relative to the principal bounding faults. All analog models of releasing stepovers developed a through-going, cross-basin fault linking the principal bounding faults.

Comparison of the basic features of these models with the Coso–Owens Lake–Indian Wells Valley structural setting shows that first-order structures correlate very well. The principal bounding faults in the Dooley and McClay (1997) model correspond to the Little Lake fault zone and an unnamed fault, or faults, in the Wild Horse Mesa area. The Airport Lake and the Coso Wash faults appear to be analogous to cross-basin faults that form in analog models of pull-apart basins. Modern seismicity and neotectonic features associated with these two faults can be traced north-northwestward through the Indian Wells Valley to the eastern end of the White Hills anticline (Fig. 2). At that point strain is transferred ~10 km west in a left (restraining) step and continues northward along the Coso Wash fault to the Haiwee Spring area, where it dies out as a well-defined surface fault. Coso Wash also terminates here as an active depositional basin. The left step across the White Hills anticline is analogous to a borderland structure, and the left-stepping, NE-trending normal faults that constitute the Coso Wash fault are analogous to terraced sidewall structures produced in the Dooley and McClay (1997) models.

Exactly how dextral shear strain on the Coso Wash cross-basin fault is transferred northward from Haiwee Spring through the remainder of the Coso Range and into the Owens Lake is unclear. Fault-related lineaments and tectonic-geomorphic features can be traced north of Haiwee Spring to the southern end of Upper Centennial Flat (Unruh and Streig, 2004). These features may represent surface deformation associated with the northern continuation of the Coso Wash fault. Carver (1970) described tight folds in the Pliocene Coso Formation on the northwestern flank of the Coso Range. These folds lie approximately along a straight-line connection between upper Coso Wash and the southern extent of the coseismic surface rupture during the 1872 earthquake (M = 7.5–7.7) on the Owens Valley fault documented by Beanland and Clark (1994). It is possible that the folding represents surface deformation associated with incipient development of a through-going strike-slip fault. Vittori et al. (1993) described surface rupture along a NW-striking fault in the northwestern Coso Range piedmont, which they attributed to the 1872 Owens Valley earthquake. If this interpretation is correct, then the southern end of the dextral Owens Valley fault approaches within ~18 km of the northern termination of the Coso Wash fault in Upper Centennial Flat. The southern Owens Valley fault is in the location of the cross-basin fault predicted by the analog models. Detailed Quaternary mapping of the "neotectonic gap" between Haiwee Spring and the southern end of the 1872 rupture on the Owens Valley fault currently is in progress to resolve this issue.

In the Dooley and McClay (1997) analog models, the cross-basin fault is the locus of maximum crustal thinning. Figure 5 is a cross section through the center of the 30° stepover model that shows a scaled 4.5-km-deep basin and 3.5-km-thick prekinematic layer. The beginning thickness of the prekinematic layer was scaled to 8 km, implying that the upper
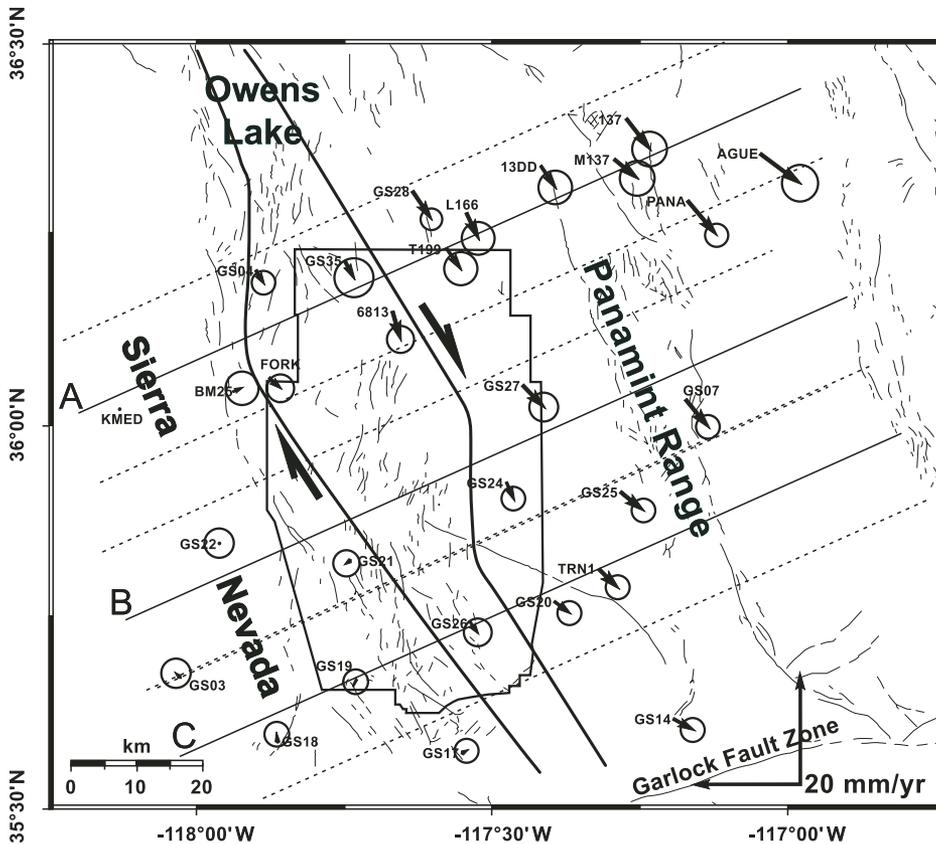

Figure 3. Results of crustal velocity determinations plotted relative to station KMED located in the southern Sierra Nevada. Data were acquired from 1993 until 2000. Global positioning system stations in the Coso Range area are located at the tip of each of the arrows. The length of the arrow shafts is proportional to the velocity, and the size of the circles is a measure of the uncertainty of the value. Locations of three cross sections shown in figure are labeled A, B, and C. Dotted lines on either side of the cross section lines define the area from which individual stations were projected to the cross section. Heavy red lines with arrows indicating sense of offset on the principal bounding faults are our interpretation of the Coso stepover.

crust has thinned by more than 50% in the most highly extended part of the model. The correlative location of the model cross section in the Coso Range is shown as A–A' on Figure 2. This suggests that the crust is thinnest in the vicinity of the Coso Wash, which coincides with the highest recorded temperature gradients (>100 °C/km) and maximum temperatures (346 °C) in the geothermal wells drilled there. Gradients of this magnitude result in temperatures of ≥350 °C, sufficient for attainment of ductility in quartz-rich rocks at depths of 3.5 km, thus supporting the contention of a shallow brittle-ductile transition.

Crustal Thinning and Basal Accommodation within the Coso Releasing Bend

A consequence of the releasing bend geometry that we interpret for the Coso Range is that crustal thinning locally accommodates distributed regional dextral transtension. The thinning mechanisms associated with metamorphic core complex formation have been discussed in terms of pure shear (necking) of the crust (Davis and Coney, 1979), simple shear in the upper crust combined with ductile deformation in the lower crust (Block and Royden, 1990), and simple shear of the entire lithosphere (Wernicke, 1981). Wernicke and Axen (1988) and Buck (1988) almost simultaneously proposed a more elaborate model for unroofing of metamorphic core complexes that involves formation of detachment faults at high angles, and subsequent rotation of the structures into a lower-angle orientation as deformation progresses. In fully exhumed metamorphic core complexes, brittle faults in the upper crust appear to sole out in the ductile lower detachment. This may be the case at Coso, where moderately dipping faults imaged on seismic reflection profiles terminate against or sole into a reflective horizon that Unruh et al. (2002b) interpreted to be the shallow brittle-ductile transition.

One of the major arguments against simple shear on listric normal faults as the mechanism for thinning the upper plate in metamorphic core complexes has been the paucity of evidence in support of the existence of seismogenic low-angle faults (e.g., Jackson, 1987; Jackson and White, 1989). It is important to emphasize that there is an extremely limited number of cases where there has been verification of seismicity on low-angle normal faults. The only fully verifiable methods known to us are where events are sufficiently large that the waveform can be modeled (Mori and Hartzell, 1990), or events from a single earthquake are aligned on a low-angle plane (Reitbrock et al., 1996). Using high-resolution cluster analysis,

A

B
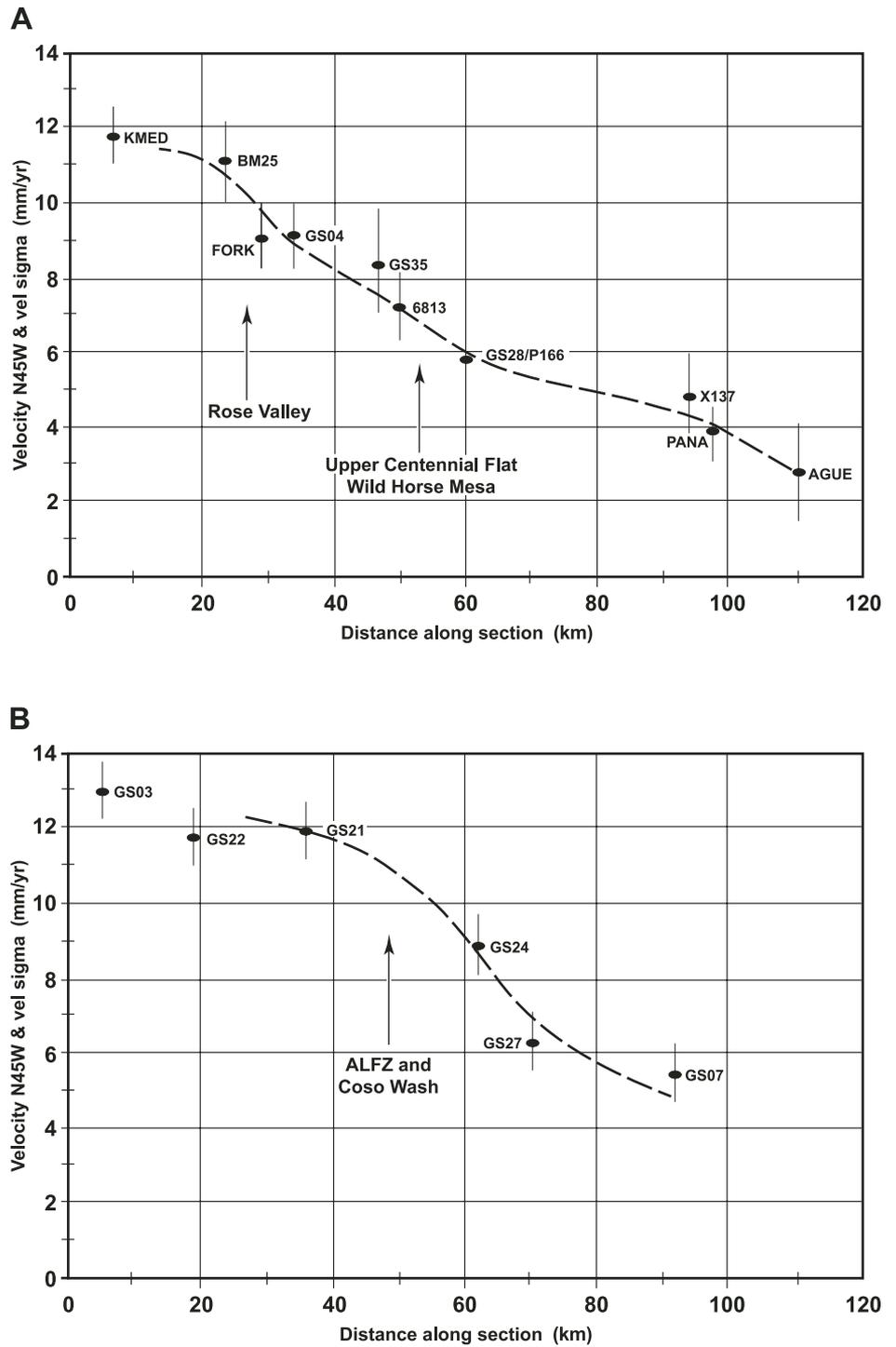
Figure 4. Cross sections of crustal velocity from precise global positioning system data. ALFZ—Airport Lake fault zone. (*Continued on following page.*)

Reitbrock et al. (1996) provided clear evidence for movement on a low-angle normal fault in a metamorphic core complex located in the western Gulf of Corinth, Greece, and Huang et al. (1996) described seven definable low-angle normal events in the southern Sierra Nevada that they attributed to primarily E-W extension. Abers (1991) and Abers et al. (1997) suggested that normal earthquake focal mechanism solutions from events in the region
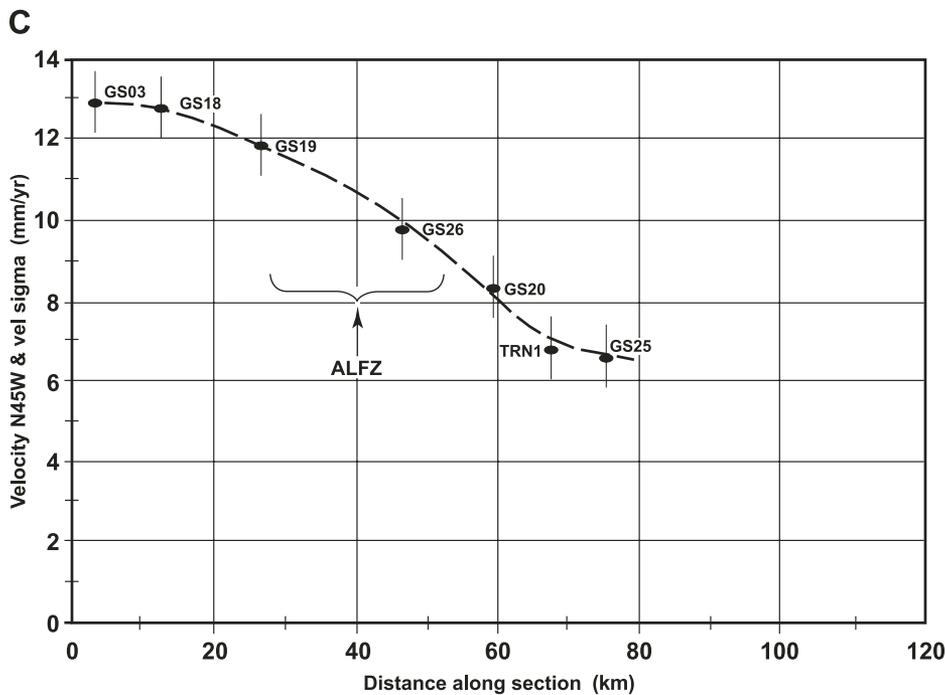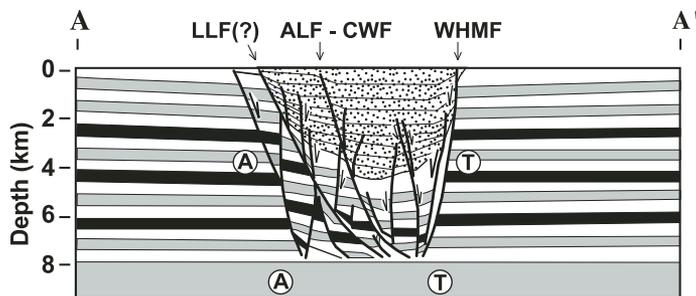
C

Figure 4 (*continued*).

Figure 5. Cross section through the Dooley and McClay (1997) 30° translational stepover model. Model depth to basement from the original surface is 8 km. Alternating dark and light bands represent prekinematic layers. Stippled layers are postkinematic layers that are added at various stages of model advancement. The "A" and "T" in the circles represent blocks moving away from and toward the viewer, respectively. Projected location of cross section A–A′ is shown on Figure 1. LLF—Little Lake fault, ALF-CWF—Airport Lake fault–Coso Wash fault, WHMF—Wild Horse Mesa fault. Little Lake fault designation is queried on this cross section because it is not clear whether it is actually that fault or the furthermost fault on the left of the figure.

and horizontal orientations. They showed that such stress rotations could occur around an actively inflating vertical dike, or they could be the result of increased mid-crustal mobility (isostatic uplift) due to thermal softening resulting from magmatic intrusion.

Alternatively, Chéry (2001) tested the hypothesis that low-angle normal faults can occur if the coefficient of friction on the fault plane is low, resulting in horizontal variations in stress and strain in the brittle crust above a metamorphic core complex that are controlled by a weak, moderately dipping normal fault acting as a "breakaway" structure. The model assumes that the coefficient of friction along the breakaway fault is ~0.1, in contrast to a coefficient of internal friction for the adjacent crust of 0.6. At a distance from the weak fault, the modeled stress is characterized by maximum tension in the horizontal plane and vertical compression, as expected for crust subjected to horizontal extension. In this example the modeled stress distribution predicts that the principal stresses locally rotate to minimize the resolved shear stress on the weak breakaway fault, favoring development of, and slip on, low-angle structures (Chéry, 2001). It is noteworthy that in the work of both Parsons and Thompson (1993) and Chéry (2001), the low-angle normal faults sole out at, or just above, the brittle-ductile transition.

In the Coso geothermal area (Fig. 2), the brittle-ductile transition is defined by the effective lower limit of seismicity and high temperature gradients in production wells (Monastero and Unruh, 2002). Figure 6 is a plot of the depth to the 95th percentile for earthquake hypocenters. These data show that beneath the geothermal area itself, the base of seismicity is quite shallow (3.5–4.0 km), and deepens abruptly to 8–10 km in all directions. A NE-SW cross section through the field (Fig. 7) shows that there is a well-defined, nearly horizontal boundary, above which brittle deformation occurs, but below which there are only scattered events. The latter are possibly due to mislocation, transient high instantaneous strain rates, or vertical fluid migration. We interpret the data as indicating that the brittle-ductile transition is elevated in the central part of the geothermal field because of the very high temperature gradients found there. Geothermal production wells have measured downhole temperatures in the 320 °C to 350 °C range at 3 km depth, sufficient for onset of crystal plasticity in quartz (Brace and Kohlstedt, 1980) at the ambient strain rates in the Coso area. Likewise, temperature gradients in these wells are in the range of 85 °C/km to 120 °C/km (Combs, 1980), substantially higher than the worldwide average of 25 °C/km, and

of the Woodlark–D'Entrecasteaux extensional province, Papua New Guinea, have at least one nodal plane with dips ranging from 10° to 35°. So, while there is not a large body of seismicity data to substantiate seismogenic low-angle normal faults, there a few examples of such activity in areas where crustal extension and high strain rates have also been documented.

In recent years investigators have conducted modeling studies to evaluate conditions under which the formation of, and slip on, low-angle faults is favored in metamorphic core complex settings. For example, Parsons and Thompson (1993) postulated that slip on low-angle faults would be mechanically favorable if the principal stresses are locally rotated away from vertical
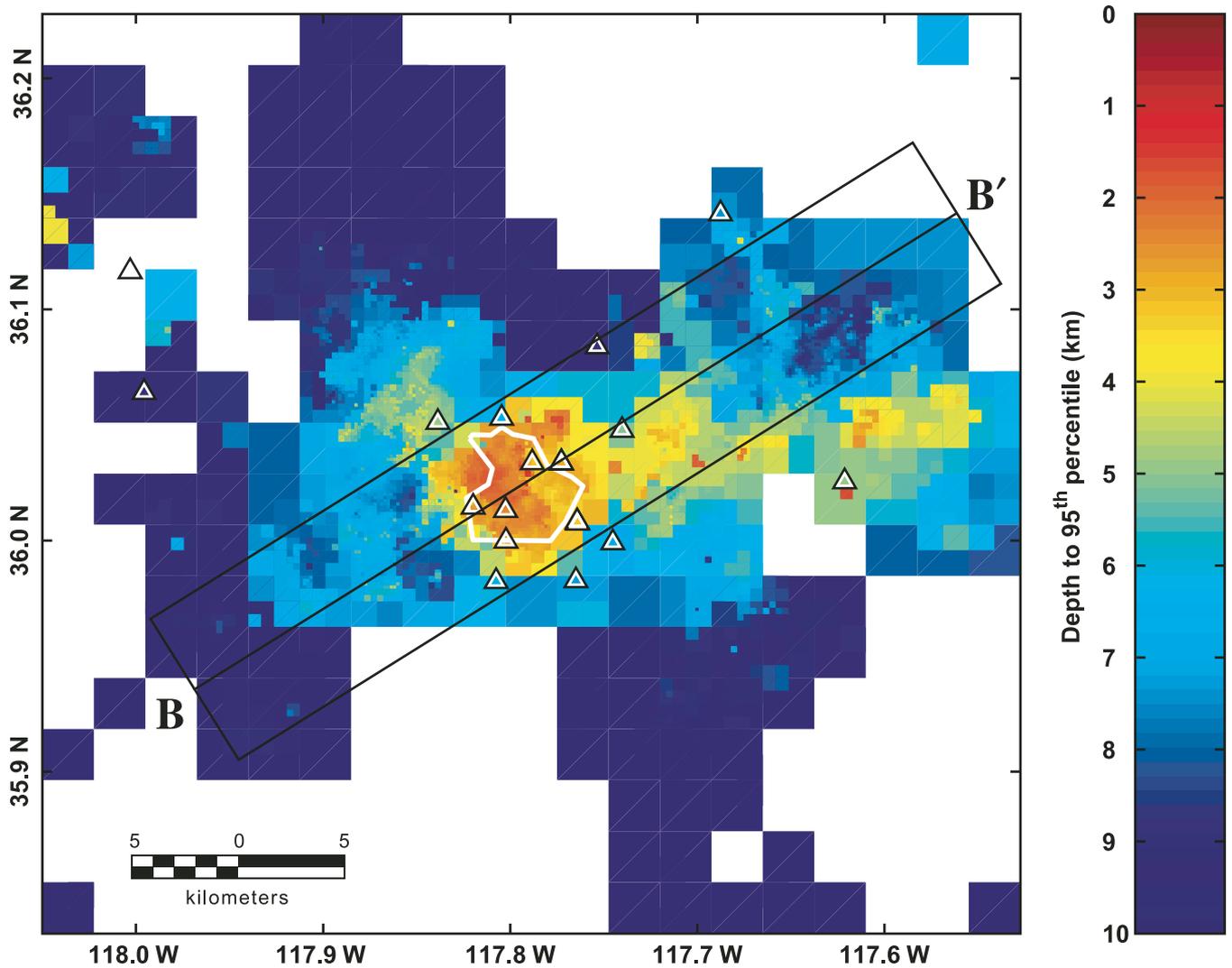
Figure 6. Maximum depth of seismicity as determined by the 95th percentile of hypocenters. Events are binned into boxes, the sizes of which are determined by event density, e.g., smaller boxes in areas of greater density. B–B′ is shown in Figure 7.

they correspond to those predicted by Fournier (1999) for a shallow (3 km) brittle-ductile transition that supports a near-surface hydrothermal system, as is found at Coso.

Because of the strong influence of the shallow brittle-ductile transition on the depth distribution of seismicity of the Coso geothermal area, we decided to test the contention of Parsons and Thompson (1993) that fault dip becomes increasingly smaller as the brittle-ductile boundary is approached. We searched the microearthquake catalog for high-quality events (6 or more triggers) for which a focal mechanism solution had been calculated that had one possible nodal plane ≤25°. The search spans the time period from 1996 until the present, because that is the part of the database in which we have

the most confidence in the accuracy of location and magnitude of events.

Results of the search showed that there were 15,170 events with magnitudes (M_L) ranging from 5.2 to –0.5 in the catalog that met these criteria. This represents 36% of the entire catalog and is an inordinately large number of such events when compared to the entire Southern California Seismic Network catalog (23.5%) for the same period of time. Wernicke (1995) investigated the recurrence interval of seismic events as a function of fault dip and found that the likelihood of an event occurring on fault planes between 30° and 60° was ten times greater than on fault planes that are <30°, a fact that he attributed principally to the efficiency of low-angle faults in dissipating resolved strain.

We performed cluster analysis on the Coso events in an attempt to isolate them onto either the vertical or horizontal nodal planes, but the results were inconclusive. The fact that more than one-third of the events recorded near the base of seismicity in the vicinity of the Coso geothermal field exhibited focal mechanisms with a low-angle nodal plane is evidence that the mechanical conditions are permissive of seismogenic slip on low-angle faults in this setting. Furthermore, results of the finite element modeling of Ofoegbu and Ferrill (1998) clearly showed that due to the inherent efficiency of low-angle normal faults in dissipating resolved strain on the fault surface, slip on listric faults can occur, but may be manifest in very small magnitude events. So, in effect, these authors
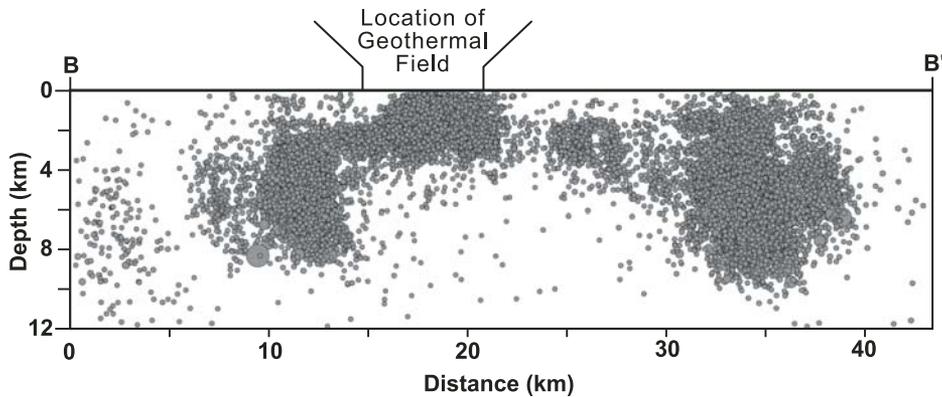
Figure 7. NE-SW cross section B–B′ showing hypocenters beneath the Coso Range for more than 40,000 events ranging in magnitude from –1 to 5.2.
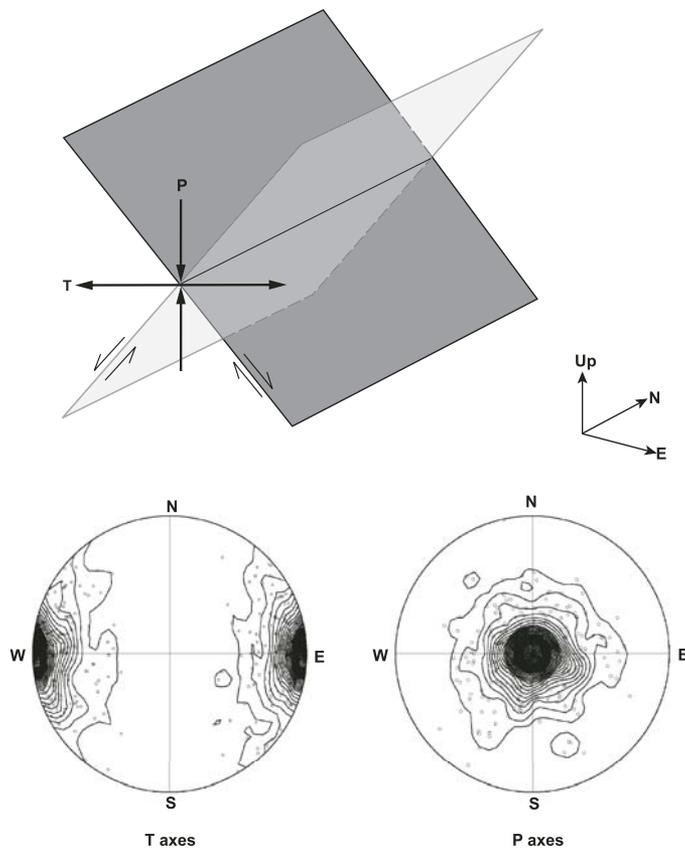

Figure 8. Relationship of P and T stress axes to moderately dipping (45°) normal fault planes, and resultant Kamb contour plots (lower-hemisphere projections). Input for the Kamb plots was generated by assuming a 45° dip on the fault plane and then randomly perturbing the data 500 times to generate a normal distribution about the pole.

establish that the absence of detectable seismic events on low-angle normal faults does not preclude their existence. In reality their detection may be a function of the sensitivity of the seismometer network that is in place.

We use Kamb plots of depth-segmented P and T axes for 921 well-constrained seismic events from within the Coso geothermal field in order to further determine if these axes are progressively rotated from vertical and horizon-

tal orientations, respectively, with depth, thus indicating that slip on low-angle normal faults is mechanically favorable. Kamb plots are used instead of the more common nodal plane representations (i.e., "beach ball diagrams") because they provide a clearer, more precise picture of changes in faulting style with depth.

Seismic P and T axes lie in a plane that is normal to the two orthogonal nodal planes of an earthquake focal mechanism. Both axes are oriented at 45° to the nodal planes with the P axis lying in the quadrants of contractile first motions about the earthquake focus, and the T axis lying in the quadrants of dilatational first motions (Cox and Hart, 1986). Anderson's (1951) theory of faulting predicted that most normal faults are initiated with dips ranging from 45° to 70° in the brittle upper crust of Earth. That would place the P and T stress axes in a more or less vertical and horizontal orientation, respectively (Fig. 8). In contrast, focal mechanisms of earthquakes associated with horizontal shear on low-angle faults would be characterized by both the P and T axes plunging ~45° in opposite directions (Fig. 9). The geometry of the latter also characterizes vertical shear on vertical faults. Thus, the orientations of P and T axes alone are not sufficient to uniquely determine whether the subvertical or subhorizontal nodal plane is the actual seismogenic shear plane.

Changes in the orientations of P and T axes with depth beneath the eastern part of the Coso geothermal field indicate that mechanical conditions systematically vary and are compatible with shearing on low-angle faults near the base of seismicity (Fig. 10). In the upper 1–2 km depth range, T axes data plotted on a lower-hemisphere, Kamb-contour diagram form well-defined horizontal maxima that are oriented approximately E-W; P axes data form a subvertical maximum (Fig. 10A). This geometry is consistent with dominantly normal slip on faults dipping ~45° to the east and west (cf. Fig. 8).

In the 2–3 km depth range, there is a mixture of orientations of P and T axes (Fig. 10B). There are two T axis maxima that plunge ~30° to the east and 30° to the northwest, and a vertical P axis maximum, both consistent with high-angle normal faulting. In addition, however, there are distinct concentrations of moderately plunging (~45°) P and T axes in the southwest and northwest quadrants of the plot. Earthquakes associated with the latter occurred by shearing on subhorizontal or subvertical faults (cf. Fig. 9).
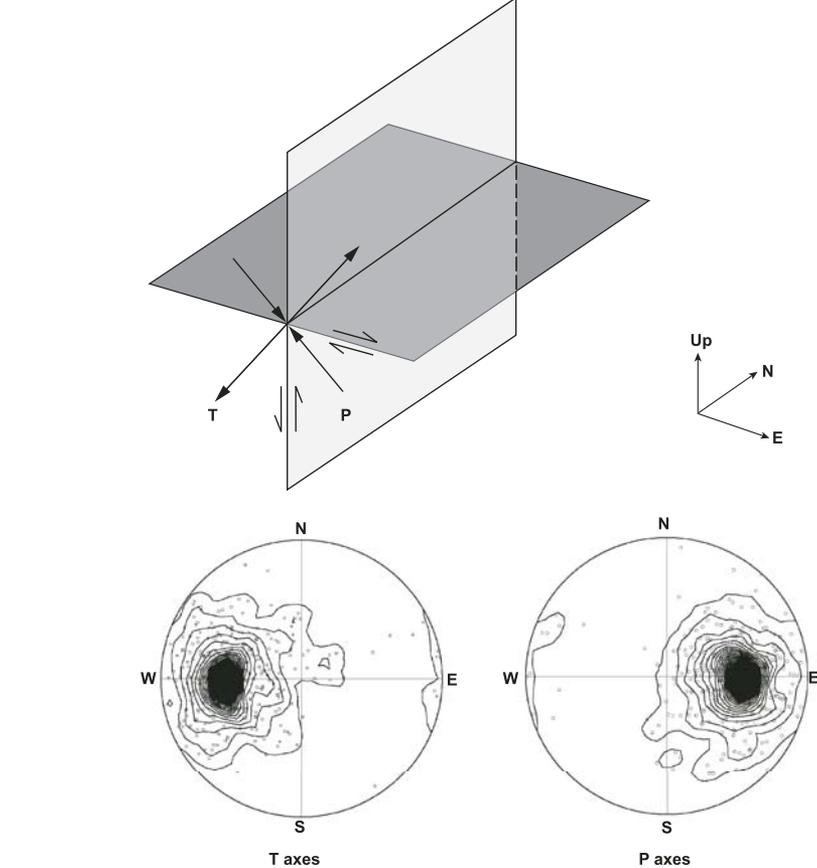
To better illustrate that the Kamb plots in Figure 10B document a mix of faulting styles in the 2–3 km depth range, we have divided all 785 events into two subsets corresponding to: (1) focal mechanisms with moderately dipping nodal planes; and (2) focal mechanisms

exhibiting high-angle and low-angle nodal planes (Fig. 11). The former are characterized by horizontal east-west T maxima and a subvertical P maximum (Fig. 11A), which are strongly expressed in the Kamb plot for all events in the 2–3 km depth range (Fig. 10B). In contrast, focal mechanisms with vertical and horizontal nodal planes are characterized by P and T axes maxima plunging to the east and west (Fig. 11B). The strong maximum of T axes plunging ~45° to the ENE in Figure 11B accounts for the distinct ENE-plunging maximum in Figure 10B. The strong maximum of P axes plunging ~45° to the WSW also is expressed as a subordinate, but distinct, maximum in Figure 10B. The dominant WSW-plunging P axis maximum in Figure 11B suggests preferred top-to-the-west motion shearing on subhorizontal fault planes.

In contrast to results from the 2–3 km depth range, Kamb plots for earthquakes in the 3–4 km depth interval reveal a clear dominance of T axes plunging ~30° toward the E and two well-defined maxima of P axes plunging ~45° toward the NW and SW (Fig. 10C). These data indicate that earthquakes in this depth range occur primarily by shear on subhorizontal faults, and/or subvertical, N-S–striking faults. There are no concentrations of subhorizontal T axes, or a maximum of subvertical P axes, to suggest that significant slip is occurring on moderately dipping faults in this depth range, as is observed in the 1–2 km depth range (Fig. 10A). The preferred westward plunge of the P axes in the 3–4 km depth range is consistent with top-to-the-west shear on subhorizontal faults, and/or east-down shear on vertical faults (Fig. 9).

We interpret the data in Figures 10A–10C to show a systematic progression in faulting style with depth beneath the eastern part of the geothermal field consistent with the findings of Parsons and Thompson (1993). Seismogenic deformation in the upper 1–2 km is characterized by horizontal WNW-ESE extension and vertical crustal thinning, and is accommodated by normal slip on NNE-SSW-striking faults that dip ~45° toward the east and west. Deformation in the 2–3 km depth range is accommodated by a mix of normal slip on moderately dipping faults and shearing on faults that are subhorizontal and/or subvertical. In the 3–4 km depth range, seismogenic deformation is accommodated primarily by shear on low-angle faults and/or subvertical faults. The trend toward increasing fraction of events on either low- or high-angle shear planes with depth is shown in Figure 3, and is also documented by the histogram in Figure 12.

This progressive change in faulting style is evidence that the mechanical conditions systematically change with proximity to the base
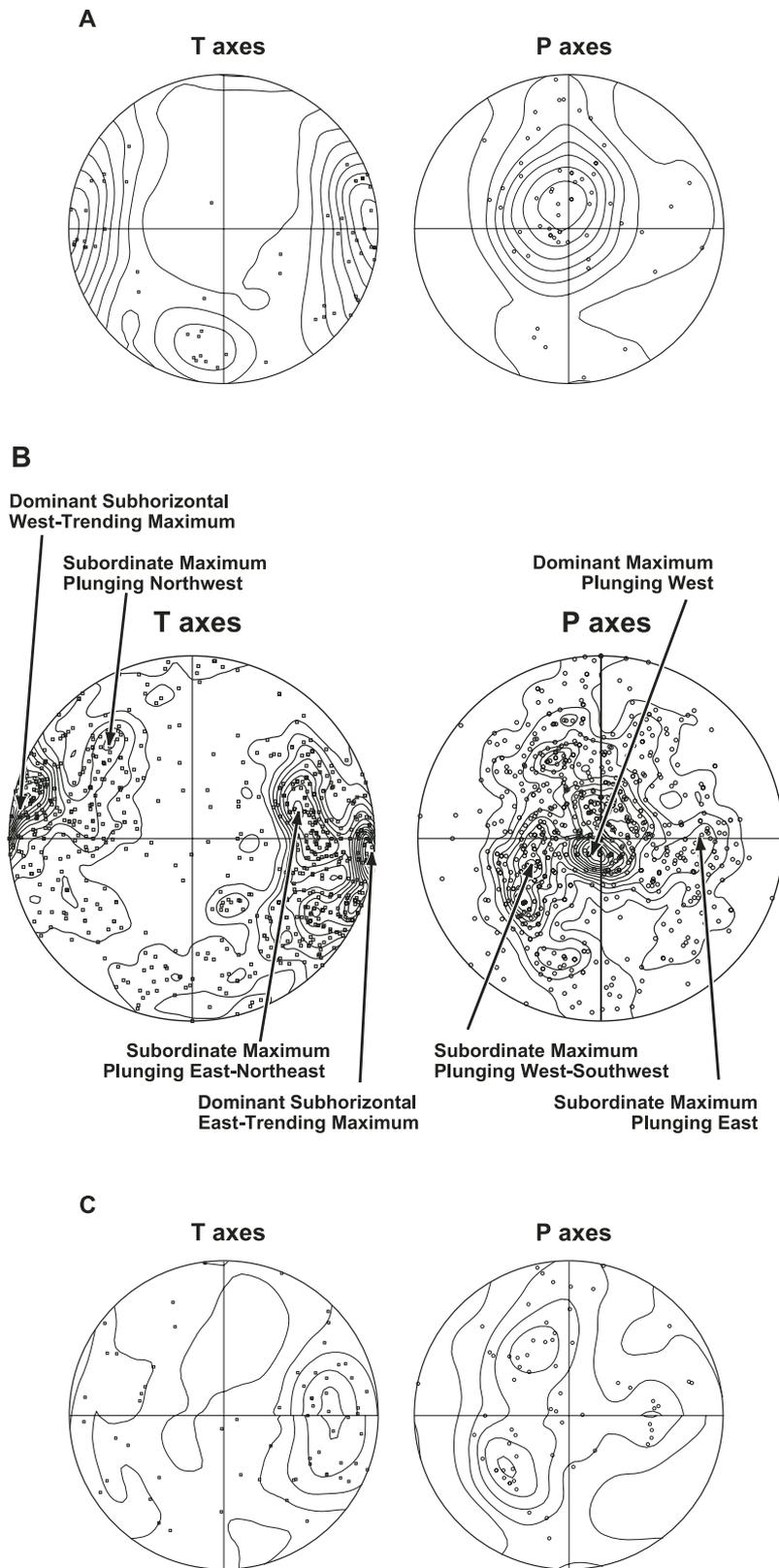
of seismicity. If the base of seismicity (~4 km in this region) is at or near the brittle-ductile transition zone, then mechanical conditions in the brittle crust directly above the zone favor shearing on subhorizontal (and subvertical) faults. The systematic change in faulting style exhibited in Figure 10 is consistent with mechanical models that predict rotation of the principal stresses away from horizontal and vertical orientations to produce significant shear stresses on subhorizontal faults in areas of detachment-style faulting (e.g., Parsons and Thompson, 1993; Chéry, 2001).

Geochemical Evidence of Crustal Thinning in the Coso Range

Results of geochemical analyses of rock, liquid, and gas samples from the Coso geothermal area provide compelling evidence of asthenospheric influence in the Pleistocene-Recent bimodal volcanic suite, relatively shallow depth to dense lower-crustal or upper-mantle type

rocks, and thermal influence of asthenospheric material. Collectively, these data support the assertion that crustal thinning in the Coso Range enabled mantle melts to reach relatively shallow depths and create the observed thermal anomaly with temperatures at 3.5–4.0 km in the brittle-ductile transition range for silicic rocks.

Radiogenic Sr and Nd isotopic data on the bimodal Pleistocene volcanic rocks and Mesozoic crystalline basement rock samples taken from the Coso geothermal area (Fig. 13) are consistent with the involvement of young, possibly asthenospheric, mantle. Basalts from Coso have isotopic values that range from +3 to +8 ε_{Nd}, and 0.703–0.7055 for $^{87}Sr/^{86}Sr$, and rhyolites have high ε_{Nd} values (avg. ~+2), and relatively low $^{87}Sr/^{86}Sr$ ratios (0.705–0.707). The highest ε_{Nd} and lowest $^{87}Sr/^{86}Sr$ basalts are indicative of a mantle source, with high time-integrated Sm/Nd and low Rb/Sr. Figure 13 shows that the Coso basalt Sr and Nd isotope values are most similar to those from the Cima volcanic field basalts, which Farmer et al. (1995) concluded

Figure 9. Relationship of P and T stress axes to flat or vertical fault planes, and resultant Kamb contour plots (lower-hemisphere projections). Input for the Kamb plots was generated by assuming a 0° dip on the fault plane and then randomly perturbing the data 500 times to generate a normal distribution about the pole.

A

T axes   P axes

B

Dominant Subhorizontal
West-Trending Maximum

Subordinate Maximum
Plunging Northwest

T axes

Dominant Maximum
Plunging West

P axes

Subordinate Maximum
Plunging East-Northeast

Dominant Subhorizontal
East-Trending Maximum

Subordinate Maximum
Plunging West-Southwest

Subordinate Maximum
Plunging East

C

T axes   P axes

Figure 10. Kamb contour plots (lower-hemisphere projections) of seismic P and T axes from the eastern Coso geothermal production area. A, B, and C represent depth intervals of 1–2 km (59 axes plotted), 2–3 km (785 axes plotted), and 3–4 km (64 events plotted), respectively. Contour interval is two sigma. See text for discussion.

were derived from a Pacific mid-ocean-ridge basalt source (i.e., asthenosphere). Some of the Coso basalts have slight enrichment in large ion lithophile and light rare earth elements (Groves, 1996) that could be inherited from Mesozoic subduction of the Farallon plate beneath the western United States. Thus, melting of young subduction-modified (?) lithosphere could also play a role in basaltic volcanism at Coso. However, these enrichments could also be explained by minor contamination of asthenosphere-derived basalt with Mesozoic crust. The spread to higher $^{87}Sr/^{86}Sr$ and lower ε_{Nd} values for the basalts is attributable to crustal contamination of high ε_{Nd}–low $^{87}Sr/^{86}Sr$ basalts, and indicates that many of the basalts did not make it to the surface unmodified from their mantle sources (Groves, 1996; Bacon and Metz, 1984).

Results of isotope analysis of Coso rhyolites show a similar mantle influence. The data are consistent with petrogenesis in closed-system fractionation, either crystallization or remelting of intermediate rocks derived from mixing of the crust and asthenospheric basalt magma (Miller et al., 1996; Miller, 1999). The occurrence of andesitic inclusions within rhyolite samples, and overlap in Nd isotopic compositions of the inclusions and the host rhyolites, suggests kinship—possibly a fractionation relationship—between an intermediate andesite magma and an evolved rhyolite magma. Regardless, the isotopic values for the Coso rhyolites shown in Figure 13 require that they have appreciable mantle-derived neodymium. Strontium isotopic composition of the Coso rhyolites is decoupled from neodymium isotopic composition in the sense that the latter has a fairly restricted range (2.5 ε_{Nd}-unit spread), whereas there is a fairly large spread in the former. This can be explained either by late-stage shallow assimilation of small amounts of strontium-rich upper-crust rocks into the very low-Sr rhyolite magmas, or hydrothermal disturbance of the Sr system (Miller et al., 1996).

Although the range of ε_{Nd} values for the Coso rhyolites is fairly restricted, there is a systematic shift with time from $\varepsilon_{Nd} = +4$ in the oldest rhyolite (ca. 1 Ma) to about +2 in the youngest, and most voluminous, rocks. Errors are ±0.3 ε_{Nd}-units, based on replicates and repeat analysis of standards. The shift is attributed to greater amounts of crustal involvement in rhyolite magma production as the system grew. Based on geobarometric analysis of phenocrysts from the Coso rhyolites, Manley and Bacon (2000) concluded that the magma chamber has been in existence for at least 1 m.y., during which time it has risen from a depth of ~10 km to a depth of ~5 km and has become hotter by at least 30 °C. Shallowing of the magma chamber would

permit longer residence time for the melts in the crust, thus increasing the likelihood of crustal contamination and a shift in the ε_{Nd} values.

Similar findings result from geochemical analysis of gas samples from the Coso field. In general, high ^{3}He content indicates a mantle or crustal origin, and high N implies a magmatic source associated with subducted sediments (Giggenbach, 1986). Results of analyses of pre-production gas samples taken from three Coso wells (51A-16, 65A-18, and 78B-6) that were unaffected by injection and from a major fuma-rolic area all show very high concentrations of ^{3}He and low N (Fig. 14). These samples plot in the field with Ascension Island, which is fed by a shallow asthenospheric source.

It was determined by Marty and Jambon (1987) that the carbon to ^{3}He (C/^{3}He) ratio does not change during mantle degassing, and generally has a value of 2×10^9, which is similar to that measured in mid-ocean-ridge basalts (MORB). Welhan et al. (1988) and Giggenbach et al. (1993) made surveys of volcanic gasses in geothermal systems in North America and the world, respectively, which show that there is a great variety of crustal ratios that have mixed with mantle sources. In order to differentiate between crustal and mantle origins, one can plot ^{3}He/^{4}He ratio (shown as R/Ra in Fig. 15) versus C/^{3}He ratio. Coso data plot in the same region as results from gas analyses from Ascen-sion Island, Yellowstone National Park, Mount Baker and Mount Lassen in the Cascade Range, and many of the volcanic fields of the Taupo volcanic zone in New Zealand (Adams, 1996). Gas constituents from all of these locations exhibit a strong asthenospheric influence.

Gravity Data and Modeling

Since 1996 we have acquired gravity data from more than 3500 locations throughout the Coso Range that have been reduced to complete Bouguer gravity values. A map of the resultant data (Fig. 16) shows that the geothermal field in the central part of the Coso Range is located on the northern flank of a long-wavelength, posi-tive 20 mGal gravity high, which is atypical of geothermal fields around the world. Most have a strong negative anomaly or show no anomaly at all, a condition that has been attributed to either reduction in the density of the country rocks as a result of hydrothermal alteration, and/or massive fracturing associated with a permeable reservoir (Chapman, 1975; Batini et al., 1985). Although the Coso reservoir has significant hydrothermal alteration, well-documented permeability, and low-density rhyolite domes on the surface, the gravity signature is still dominated by the long-wavelength high, indicating the influence of a
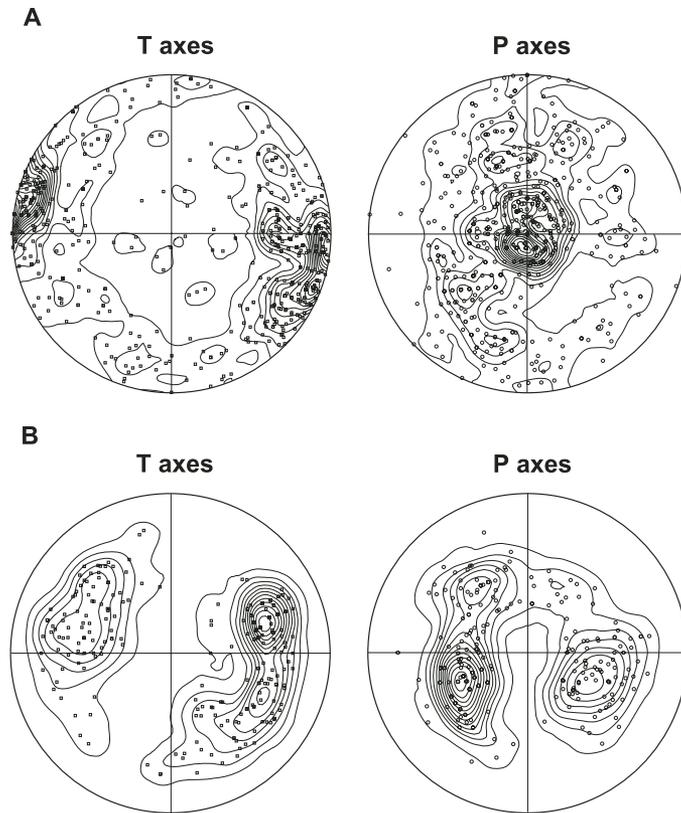
Figure 11. Kamb contour plots (lower-hemisphere projections) of seismic P and T axes from the 2–3 km depth range, eastern Coso geothermal production area. (A) shows only the events that occur on moderately dipping faults (546 axes plotted). (B) shows events that occur on subhorizontal or subvertical faults (239 axes plotted). Contour interval is two sigma. See text for full discussion.
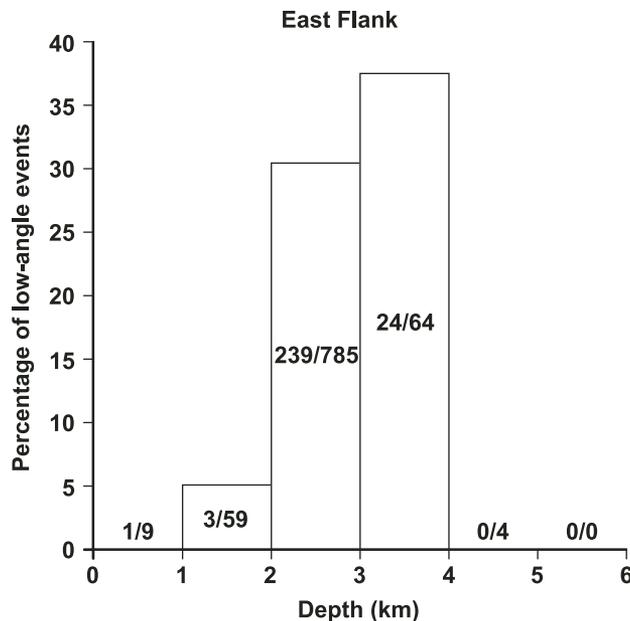
Figure 12. Histogram showing fraction of low-angle ($\leq 25°$) events as a function of depth beneath the eastern Coso geothermal production area. Total number of events is 921. Num-bers represent the fraction of low-angle events in each depth interval. If there were fewer than 10 events in one depth interval, they were not plotted.
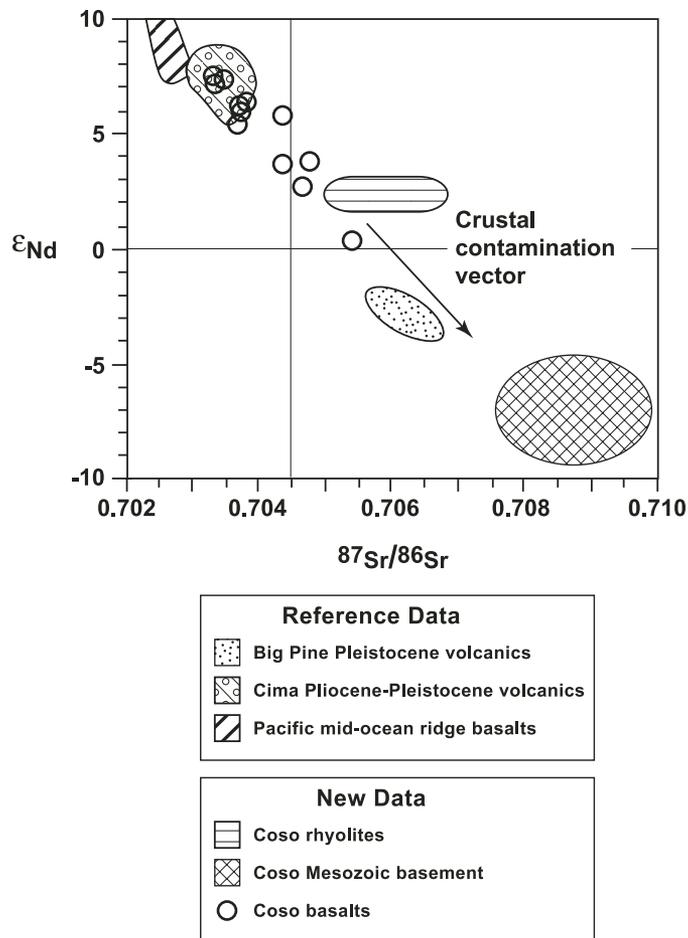
Figure 13. Plot of ε_{Nd} vs. $^{87}Sr/^{86}Sr$ for Pleistocene-Recent volcanic rocks from the Coso Range. The Big Pine data are taken from Ormerod et al. (1988), the Cima data from Farmer et al. (1995), and the Pacific mid-ocean-ridge basalt (MORB) field data from White et al. (1987).

The 2.90 g/cm^3 material represents a dike complex composed of mafic material intruded into lower-density, upper-crustal rocks, and the 3.15 g/cm^3 diapir is localized ultramafic asthenospheric material intruded into the space beneath the highly extended Coso core complex. The 3.05 g/cm^3 rocks represent mafic cumulates left over from the fractional crystallization process that formed the Pleistocene rhyolites found on the surface at Coso. This is not an unusual circumstance in areas of highly extended crust. Metcalf et al. (1995) and Faulds et al. (1995) described mafic cumulates derived from asthenospheric material in the root of the fully exhumed Mount Perkins pluton located in the northern Colorado River extensional corridor. These investigators observed that crustal thinning associated with core complex formation caused asthenospheric material that underwent fractional crystallization and formation of mafic cumulates to intrude or underplate the distended crust. Based on hornblende geobarometry, Metcalf et al. (1995) determined that these high-density cumulates reached depths of 5–7 km, similar to the 6-km-deep density contrast in our model. Inserting the 3.05 g/cm^3 mafic cumulates in the 6–12 km depth range enables us to assign a very reasonable density value of 2.80 g/cm^3 to the mixed complex. Regardless of what density values are assigned to crustal rocks in the upper 5 km of the Coso area, two requirements must be met in order for the model to approximate the observed data: (1) the Moho must be bowed upward to bring the high-density (3.30 g/cm^3) body beneath the central part of the field nearer to the surface; and (2) the entire intrusion must have a diapiric shape.

high-density rock mass at depths greater than the production reservoir.

Outcrops of Mesozoic plutonic basement rocks in the Coso Range have a wide range of densities and vary in composition from leucogranite to gabbro with a common occurrence of rocks referred to by Whitmarsh (1998) as mixed complex. The latter are an intimate mixture of felsic and mafic components that have densities ranging from 2.75 to 2.95 g/cm^3, depending on the percentage of each end member in the sample. Reasonable density values for the rocks in the Coso Range vary from 2.65 g/cm^3 for leucogranite to 3.0 g/cm^3 for gabbro (Telford et al., 1976; Carmichael, 1990). Using percentages of the various rock types encountered in drill holes in the Coso geothermal area as a guide, we believe that a reasonable average density for the mixed complex is 2.80 g/cm^3. The mixed complex and the transition zone in our gravity model correspond to the stratified (granite over diorite) pluton that is exposed in the exhumed

Black Mountains metamorphic core complex (Serpa and Pavlis, 1996).

We prepared a 2½-D model of the gravity data for the Coso field along a NW-SE–oriented cross section through the main production area (Fig. 17). Based on the findings of Jones et al. (1994) and Fliedner et al. (2000), we assumed that the Moho beneath Coso was bowed upward to a depth of 28 km in the central part of the field, dropping off to a depth of 36 km at the margins. Because of the shape of the long-wavelength gravity anomaly and the steep gradients that form its boundary, we have chosen to model the mass using the layered mafic ore bodies that have been studied throughout the world as a template, i.e., the Skaergaard intrusion, the Bushveld complex, and the Musk Ox complex (Cox and Singer, 1987). Our model fits the field data when a transition zone consisting of 2.90 g/cm^3 material is inserted above the 6 km level and is underlain by high-density (3.05 g/cm^3) material.

DISCUSSION

Metamorphic Core Complex or Not?

A nascent metamorphic core complex may not conveniently exhibit all of the features of its fully exhumed cousins, but there are fundamental characteristics that should be discernable to distinguish core complexes from other extensional structures. First, there has to be a mechanism that localizes extension of the crust, such as the dextral strike-slip releasing-bend found at Coso. This geometry requires that extensional rates across the stepover be comparable to slip rates on the bounding strike-slip faults. In the case of Coso, GPS data suggest that these rates may approach 6 mm/yr (McClusky et al., 2001). If such rates are sustained over a geologically significant period of time, extension of many kilometers to tens of kilometers can accumulate in several million years. Analog modeling (Dooley and McClay, 1997; Rahe et al., 1998;

Sims et al., 1999) of such systems replicates many of the structures that we see in the Coso Range, including the cross-basin Airport Lake–Coso Wash fault, and supports the notion of localized crustal thinning within the stepover (Fig. 18). Seismicity in the Coso Range and surrounding areas verifies the sense of offset on the bounding faults and the cross-basin fault consistent with the dextral strike-slip releasing-bend geometry.

Based on the data presented herein, we contend that the mechanism for compensatory crustal thinning of the upper crust in the Coso geothermal area is a combination of high-angle (45–60° dip) and low-angle (<30° dip) normal faulting. This is consistent with numerous models of metamorphic core complexes (cf. Gans et al., 1985) wherein deformation of the upper (supradetachment) plate deforms in a brittle manner, as suggested by Block and Royden (1990) and the modeling work of Brun et al. (1994). Closer to the base of the zone of seismicity, there is an inordinately large number of events that have one low-angle nodal plane, which we propose is the manifestation of normal faults that are soling out against the brittle-ductile transition (Gans et al., 1985; Parsons and Thompson, 1993).

Furthermore, the pronounced convexity of the seismic-aseismic boundary beneath Coso is also consistent with models of the shape of the detachment surface (Brun et al., 1994) in developing core complexes (Fig. 1). Parsons and Thompson (1993) (Fig. 1) showed a "zone of intrusion" that pushed the brittle-ductile transition upward, creating horizontal extensional strain, heating the country rock, and causing thermal softening. Because of this heating, they contend that stress axes were rotated away from vertical, thus favoring propagation of low-angle normal faults in the brittle upper crust. This is completely analogous to the Coso geothermal situation, and is supported by our analysis of changes in the orientation of seismic P and T axes with depth. Based on a comprehensive receiver function study of the Coso area, Wilson et al. (2003) postulated the presence of a magma chamber at a depth of ~5 km beneath the geothermal production area analogous to the aforementioned "zone of intrusion" that could explain the domed shape of the brittle-ductile transition seen in Figure 7 of this paper. The block model shown in Figure 18 is very similar in structure to the model of the now fully exhumed Black Mountains metamorphic core complex described by Serpa and Pavlis (1996) (Fig. 2).

One of the most important aspects of the Coso system supporting our hypothesis (that it is a nascent metamorphic core complex) is
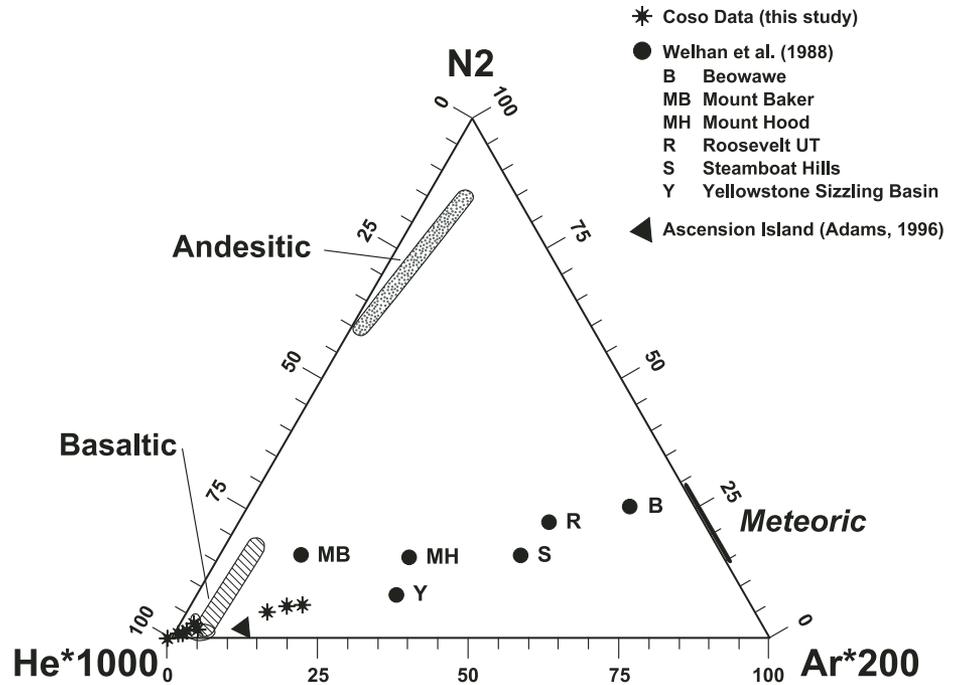
Figure 14. Ternary diagram showing the molecular ratios of N_2, Ar, and He in geothermal production waters from the Coso field. Locations of the andesite and basalt fields are taken from Giggenbach (1992). The composition of other geothermal fluids from the western United States is shown for comparison (data from Welhan et al., 1988).
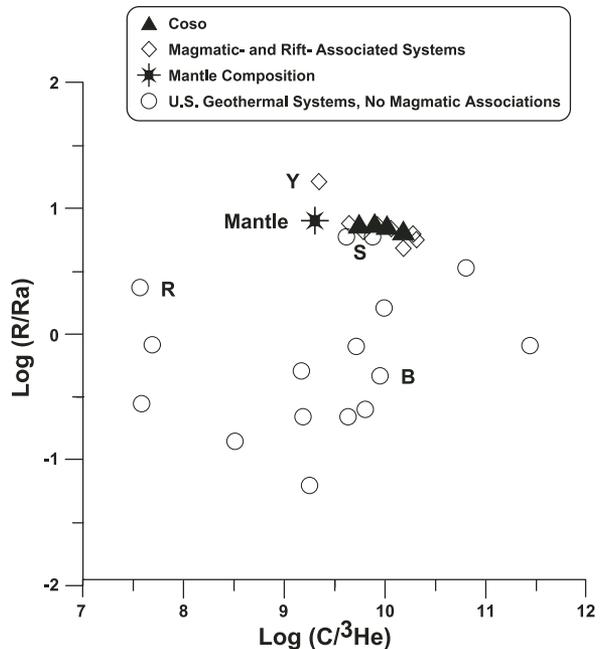
Figure 15. ^{3}He/^{4}He (R/Ra) versus the ratio of carbon to ^{3}He in Coso water, spreading centers, rift zones, and geothermal systems, some associated with volcanism or magma and some not. The magmatic and rift-associated systems include Ascension Island (Adams, 1996), Yellowstone (Y), Mt. Baker, Mt. Lassen, Guaymas Basin hydrothermal vents, Cerro Prieto, and Long Valley (Welhan et al., 1988). The mantle composition was taken from Marty and Jambon (1987). Three of the U.S. geothermal systems are noted because they are in the Basin and Range province: Roosevelt Hot Springs, Utah (R), Beowawe, Nevada (B), and Steamboat Hills, Nevada (S).
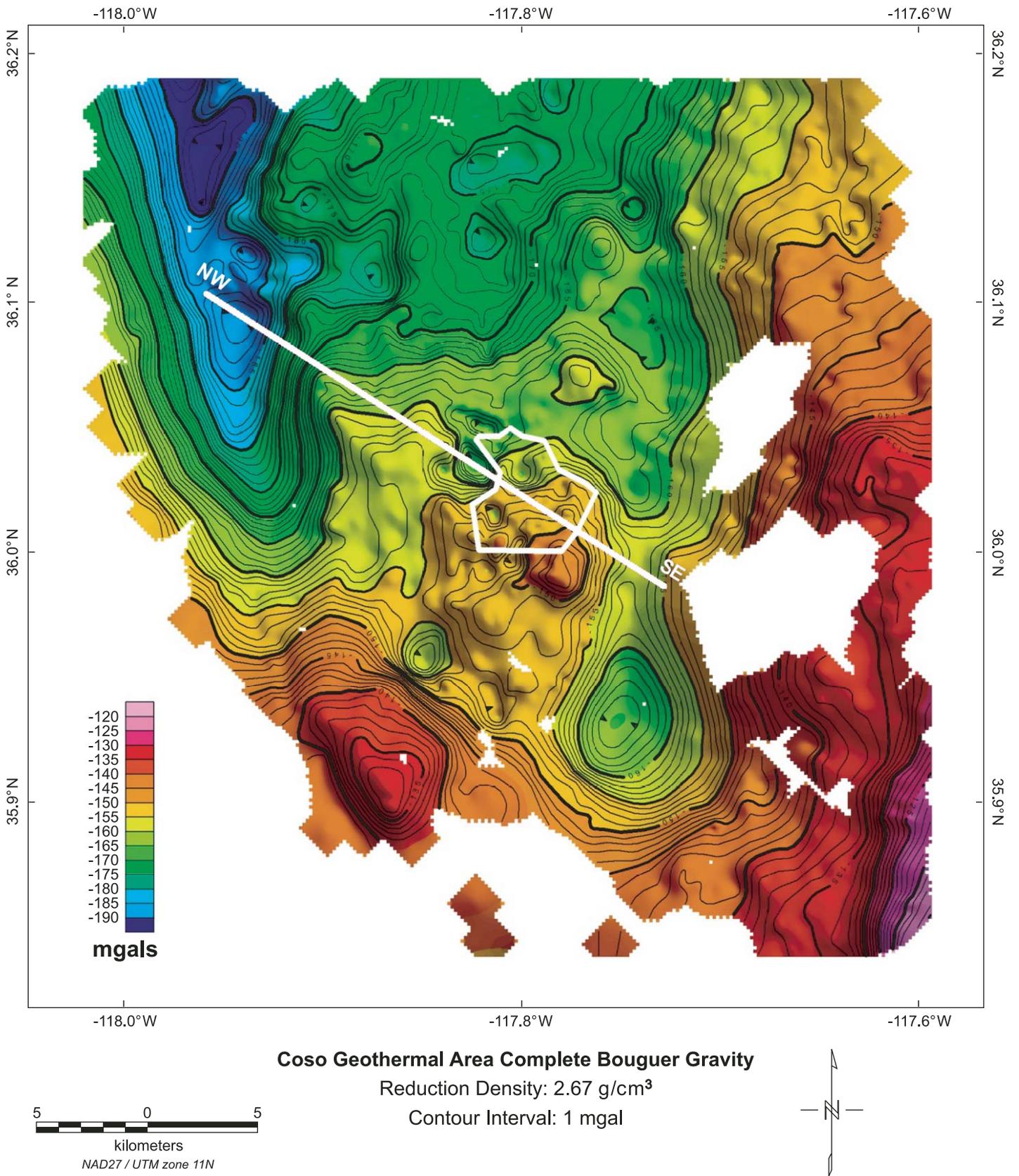
Coso Geothermal Area Complete Bouguer Gravity

Reduction Density: 2.67 g/cm³

Contour Interval: 1 mgal

NAD27 / UTM zone 11N

Figure 16. Complete Bouguer gravity map of the Coso Range based on 3500 stations. Contour interval is 1 mGal. Reduction density is 2.67 g/cm³. Data were acquired using a Scintrex Model CG3M gravimeter. Spatial coordinates were determined using a Trimble GPS 4000 series receiver. Coso geothermal area is outlined in white.
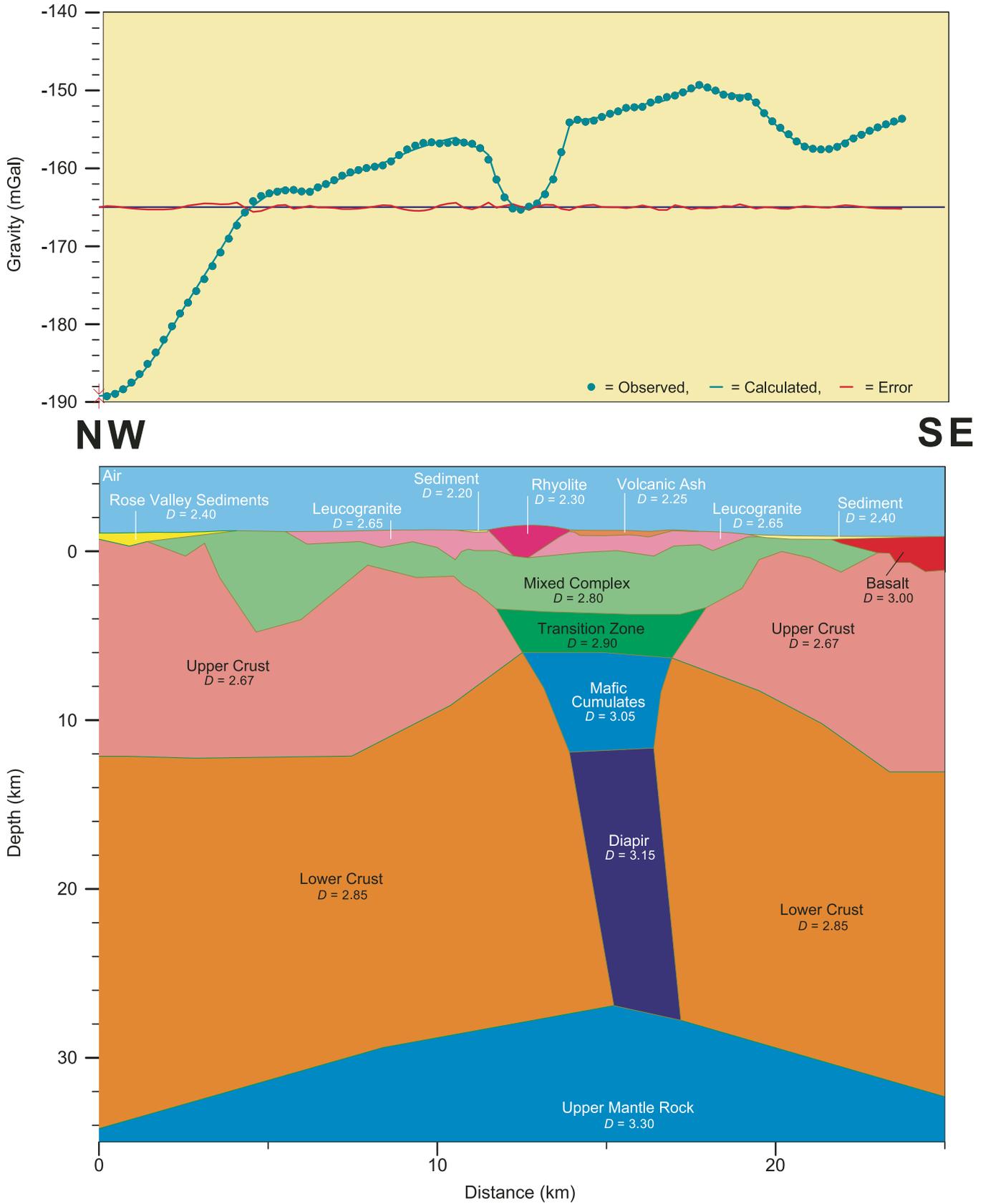
Figure 17. A 2½D model of the Coso gravity data along a NE-SW cross section (see Fig. 16 for location). The model shown in the lower half of the figure was prepared with GM-SYS® modeling software. The upper half of the figure superposes the observed gravity measurements (circles) with the calculated gravity profile from the model (solid line). Vertical exaggeration is 0.5. *D* is Density.

the very youthful volcanism represented by the bimodal suite of rhyolite and basalt. This young volcanism provides the heat engine for elevating the brittle-ductile transition to shallow depths, softens the crust, thus facilitating ductile deformation in the lower plate, and causes the stress axes to be rotated away from vertical.

The strong asthenospheric signature in the rocks and fluids from the Coso stepover is compelling evidence of passive advection of asthenosphere in the space that is created by thinning of the middle and upper crust (Martinez et al., 1999). Strontium isotope ratios and ε_{Nd} in Coso rocks both indicate a direct connection to an asthenospheric source, as do helium isotope signatures of geothermal fluids. Percentages of helium and argon and the nature of the isotopes in gas samples are both characteristic of material found in a mid-ocean-ridge environment that has a direct feed from the mantle. These geochemical signatures are attributable to crustal thinning that has permitted intrusion or underplating of dense, asthenospheric material at depths as shallow as 15–25 km, conductive melting of shallower (5–10 km depth) rocks, and elevation of the brittle-ductile transition (Fig. 17). Our gravity data modeling suggests that the locus of these phenomena is coincident with the shallowest depth to the brittle-ductile transition.

Because the Coso structure is still in its formative stages, the detachment fault separating highly metamorphosed and igneous lower-plate rocks from upper-plate rocks, which is characteristic of fully exhumed metamorphic core complexes, is not yet exposed. We suggest it exists at a depth of 4–6 km beneath the central part of the Coso Range based on several lines of evidence. First, the base of seismicity (i.e., the lower limit of brittle faulting) is ~4–5 km beneath Coso. High temperature gradients associated with the geothermal production wells in the central part of the structure are more than sufficient to produce greenschist facies metamorphism and mylonitic structures at 4 km depth, similar to what is determined from pressure-temperature studies of exhumed core complexes (e.g., Henry and Dokka, 1992). Thus, one could reasonably expect that when the Coso basal detachment structure finally is exposed at the surface, it will exhibit the same types of features as found in other fully exhumed core complexes.

When Did the Coso Metamorphic Core Complex Begin Forming?

We assume that initiation of the Coso metamorphic core complex was coincident with onset of dextral shearing along the eastern front of the Sierra Nevada. There is no precise date for when this occurred, but Monastero et al. (2002) estimated that the transition to NW-directed transtension began sometime between 3 Ma and 2 Ma, based on the opening of the Coso Wash (Duffield et al., 1980) and a number of other factors. The onset of dextral shear in the Indian Wells Valley–Coso Range may have occurred as a result of an abrupt westward shift in the locus of deformation along the entire eastern margin of the Sierra Nevada, thus narrowing the rigid Sierran microplate (Jones et al., 2004). Stockli et al. (2000) and Trexler et al. (2000) also concluded that the onset of dextral strike-slip faulting took place at this same time in the nearby Owens Valley.

Pressure-temperature studies of core complexes in the southwestern United States have shown that once denudation begins, metamorphic core complexes are fully exhumed in a matter of 5–8 m.y. (e.g., Livaccari et al., 1995). For example, Henry and Dokka (1992) showed that for the Central Mojave core complex, the brittle-ductile transition moved upward from a depth of ~20 km to the surface in 5 m.y. Similarly, Holm et al. (1993) showed that the Black Mountains metamorphic core complex was fully exhumed in 5–6 m.y. In the case of the Central Mojave metamorphic core complex, the exhumation rate of the lower-plate rocks was ~4 mm/yr, which is comparable to the GPS-measured rate of distributed dextral shear through the Coso Range (i.e., ~6 mm/yr; McCluskey et al., 2001). Using these examples, and the results of the Manley and Bacon (2000) geobarometric work
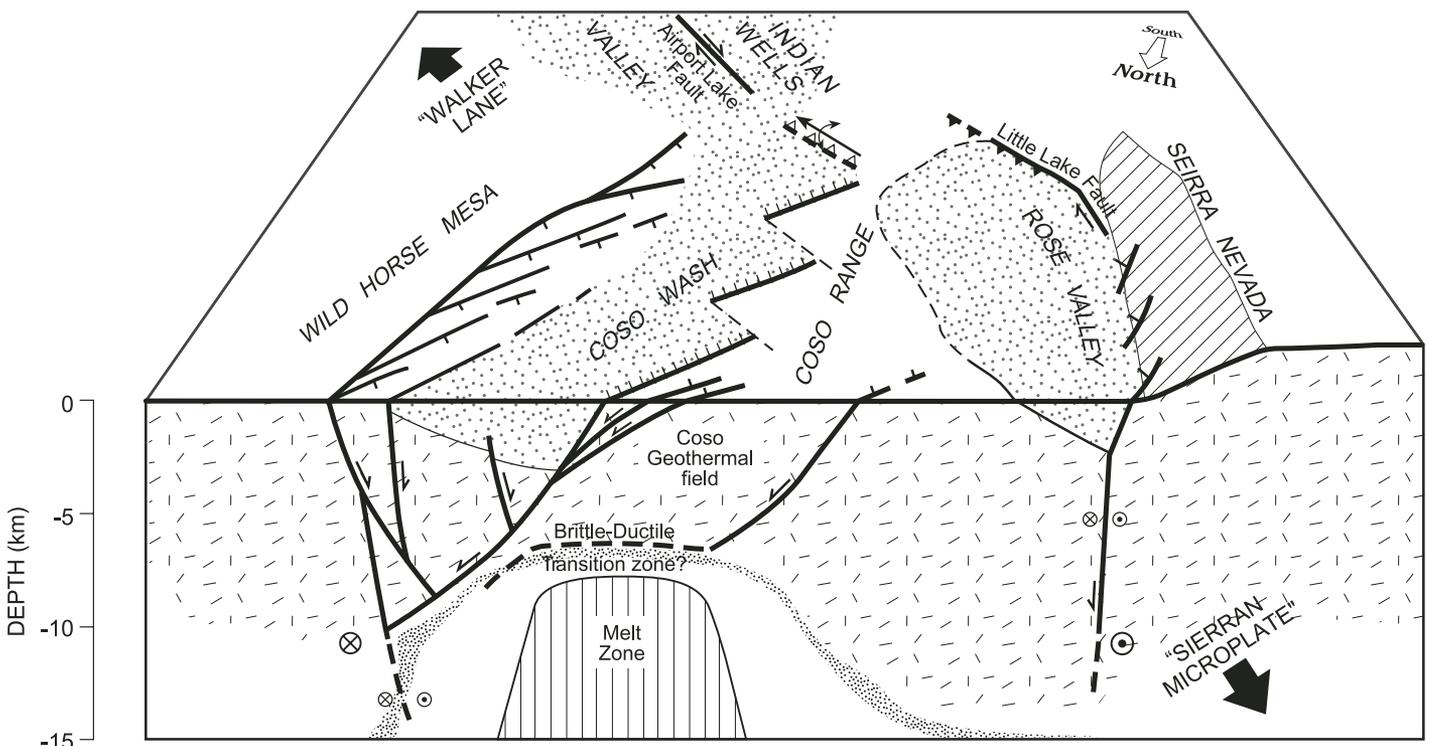

Figure 18. Three-dimensional block diagram of the nascent Coso metamorphic core complex.

that shows the Coso reservoir has been heating over the past million years, we conclude that the Coso core complex is not yet mature and will continue to be an actively forming structure for at least the next 2–4 m.y.

CONCLUSIONS

The active Coso geothermal field is located in a releasing bend of the dextral strike-slip fault system located along the eastern margin of the Sierra Nevada. Based on several lines of evidence, we conclude that this releasing bend hosts a nascent metamorphic core complex.

The structural and tectonic setting of the Coso field necessitates crustal thinning to accommodate horizontal plane-strain transtension. That crustal thinning is accomplished by brittle faulting on high-angle and low-angle normal faults in the upper 4 km of the crust. At that depth, temperatures are sufficiently high that the rocks appear to go into a ductile state based on the seismic-aseismic boundary. Normal faults above this shallow brittle-ductile transition appear to become listric with depth based on seismotectonic analysis of focal mechanism solutions. The geometry of the shallow brittle-ductile transition and the listric faults is analogous to detachment zones in fully exhumed metamorphic core complexes.

The combination of a strong positive gravity anomaly and a strong asthenospheric signature in isotopic analytical results for rocks and gases from the geothermal field attests to the close proximity to asthenospheric material in the mid-crust. Gravity modeling shows that there must be high-density (3.3 g/cm³) mafic material in the middle crust, which we interpret as cumulates from fractional crystallization of magmas that formed the bimodal Pleistocene volcanic suite found at Coso.

We propose that the Coso metamorphic core complex is in a very immature stage based on the active tectonic setting, the very shallow brittle-ductile transition, and the fact that the reservoir appears to be heating with time. It is postulated that the Coso metamorphic core complex could continue to evolve for another 2 to 4 m.y. before typical core complex–type structures are brought to the surface.

REFERENCES CITED

Abers, G.A., 1991, Possible seismogenic shallow-dipping normal faults in the Woodlark-D'Entrecasteaux extensional province, Papua New Guinea: Geology, v. 19, p. 1205–1208, doi: 10.1130/0091-7613(1991)0192.3.CO;2.

Abers, G.A., Mutter, C.Z., and Fang, J., 1997, Shallow dips of normal faults during rapid extension: Earthquakes in the Woodlark-D'Entrecasteaux rift system, Papua New Guinea: Journal of Geophysical Research, v. 102, p. 15,301–15,317, doi: 10.1029/97JB00787.

Adams, M.C., 1996, Chemistry of fluids from Ascension #1, a deep geothermal well on Ascension Island: South Atlantic Ocean: Geothermics, v. 25, p. 561–579.

Anderson, E., 1951, The dynamics of faulting: London, Oliver and Boyd, 206 p.

Argus, D.F., and Gordon, R.G., 2001, Present tectonic motion across the Coast Ranges and San Andreas fault system in central California: Geological Society of America Bulletin, v. 113, p. 1580–1592, doi: 10.1130/0016-7606(2001)1132.0.CO;2.

Armstrong, R.L., 1968, Mantled gneiss domes in the Albion Range, southern Idaho: Geological Society of America Bulletin, v. 79, p. 1295–1314.

Armstrong, R.L., 1972, Low-angle (denudation) faults, hinterland of the Sevier orogenic belt, eastern Nevada and western Utah: Geological Society of America Bulletin, v. 83, p. 1729–1754.

Bacon, C.R., and Metz, J., 1984, Magmatic inclusions in rhyolites, contaminated basalts, and compositional zonation beneath the Coso volcanic field: Contributions to Mineralogy and Petrology, v. 85, p. 346–365, doi: 10.1007/BF01150292.

Bacon, C.R., Giovannetti, D.M., Duffield, W.A., Dalrymple, G.B., and Drake, R.E., 1982, Age of the Coso Formation, Inyo County, California: U.S. Geological Survey Bulletin 1527, p. 1–18.

Batini, F., Bertini, G., Gianelli, G., Pandeli, E., Puxeddu, M., and Villa, I.M., 1985, Deep structure, age, and evolution of the Larderello-Travale geothermal field: Geothermal Resources Council Transactions, v. 9, part 1, p. 253–259.

Beanland, S., and Clark, M.M., 1994, The Owens Valley fault zone, eastern California, and surface faulting associated with the 1872 earthquake: U.S. Geological Survey Bulletin 1982, 29 p.

Beratan, K.K., 1996, Reconstructing the history of Basin and Range extension using sedimentology and stratigraphy: Geological Society of America Special Paper 303, 212 p.

Bhattacharyya, J., Gross, S., Lees, J., and Hasting, M., 1999, Recent earthquake sequences at Coso: Evidence for conjugate faulting and stress loading near a geothermal field: Seismological Society of America Bulletin, v. 89, p. 785–795.

Block, L., and Royden, L.H., 1990, Core complex geometries and regional scale flow in the lower crust: Tectonics, v. 9, p. 557–567.

Brace, W.F., and Kohlstedt, D.L., 1980, Limits on lithospheric stress imposed by laboratory experiments: Journal of Geophysical Research, v. 85, p. 6248–6252.

Brun, J., Sokoutis, D., and van den Driesche, J., 1994, Analog modeling of detachment fault systems and core complexes: Geology, v. 22, p. 319–322, doi: 10.1130/0091-7613(1994)0222.3.CO;2.

Buck, W.R., 1988, Flexural rotation of normal faults: Tectonics, v. 7, p. 959–973.

Buck, W.R., 1991, Modes of continental extension: Journal of Geophysical Research, v. 96, p. 20,161–20,178.

Cappetti, G., Celati, R., Cigni, U., Squarci, P., Stefani, G., and Taffi, L., 1985, Development of deep exploration in the geothermal areas of Tuscany, Italy, in, Stone, C., ed., International Symposium on Geothermal Energy: Davis, California, International Volume, Geothermal Resources Council, p. 303–309.

Carmichael, R.S., 1990, Practical handbook of physical properties of rocks and minerals: Boca Raton, Florida, CRC Press, Inc., 741 p.

Carver, G.A., 1970, Quaternary tectonism and surface faulting in the Owens Lake basin, California: Technical Report AT-2, prepared for the Mackay School of Mines, University of Nevada, Reno, 103 p., plus appendix.

Chapman, R.H., 1975, Geophysical study of the Clear Lake region, California: California Division of Mines and Geology Special Report 116, 23 p.

Chéry, J., 2001, Core complex mechanics: From the Gulf of Corinth to the Snake Range: Geology, v. 29, p. 439–442, doi: 10.1130/0091-7613(2001)0292.0.CO;2.

Christiansen, R.L., 1989, Volcanism associated with post-Laramide tectonic extension in the western U.S., in Continental magmatism: Rome, Italy, International Association of Volcanology and Chemistry of the Earth's Interior, p. 51.

Combs, J., 1980, Heat flow in the Coso geothermal area, Inyo County, California: Journal of Geophysical Research, v. 85, p. 2411–2424.

Coney, P.J., 1974, Structural analysis of the Snake Range "décollement," east-central Nevada: Geological Society of America Bulletin, v. 85, p. 973–978, doi: 10.1130/0016-7606(1974)852.0.CO;2.

Coney, P.J., and Harms, T.A., 1984, Cordilleran metamorphic complexes: Cenozoic extensional relics of Mesozoic compression: Geology, v. 12, p. 550–554, doi: 10.1130/0091-7613(1984)122.0.CO;2.

Cox, A., and Hart, R.B., 1986, Plate tectonics: How it works: Palo Alto, California, Blackwell Scientific Publications, 392 p.

Cox, D.P., and Singer, D.A., 1987, Mineral deposit models: U.S. Geological Survey Bulletin 1693, 379 p.

Crittenden, M., Jr., Coney, P.J., and Davis, G., 1978, Tectonic significance of metamorphic core complexes in the North American cordillera: Geology, v. 6, p. 79–80, doi: 10.1130/0091-7613(1978)62.0.CO;2.

Davis, G.A., and Lister, G.S., 1988, Detachment faulting in continental extension: Perspectives from the southwestern U.S. cordillera, in Clark, S.P., Jr., Burchfiel, B.C., and Suppe, J., eds., Processes in continental lithospheric deformation: Geological Society of America Special Paper 218, p. 133–159.

Davis, G.H., 1975, Gravity-induced folding of a gneiss dome complex, Rincon Mountains, Arizona: Geological Society of America Bulletin, v. 86, p. 979–990, doi: 10.1130/0016-7606(1975)862.0.CO;2.

Davis, G.H., 1977, Characteristics of metamorphic core complexes, southern Arizona: Geological Society of America Abstracts with Programs, v. 9, no. 7, p. 944.

Davis, G.H., and Coney, P.J., 1979, Geologic development of the Cordilleran metamorphic core complexes: Geology, v. 7, p. 120–124.

Davis, J., and Hawkesworth, C.J., 1993, The petrogenesis of 30–20 Ma basic and intermediate volcanics from the Mogollon-Datil volcanic field, southwestern New Mexico, USA: Contributions to Mineralogy and Petrology, v. 115, p. 165–183, doi: 10.1007/BF00321218.

Dixon, T.H., Miller, M.M., Farina, F., Wang, H., and Johnson, D., 2000, Present-day motion of the Sierra Nevada block and some tectonic implications for the Basin and Range Province: North American cordillera: Tectonics, v. 19, p. 1–24, doi: 10.1029/1998TC001088.

Dooley, T., and McClay, K., 1997, Analog modeling of pull-apart basins: American Association of Petroleum Geologists, v. 81, p. 1804–1826.

Duffield, W.A., and Bacon, C.R., 1981, Geologic map of the Coso volcanic field and adjacent areas, Inyo County, California: U.S. Geological Survey Miscellaneous Investigations Series Map I-1200, scale 1:50,000.

Duffield, W.A., Bacon, C.R., and Dalrymple, G.B., 1980, Late Cenozoic volcanism, geochronology, and structure of the Coso Range, Inyo County, California: Journal of Geophysical Research, v. 85, p. 2381–2404.

Evernden, J.F., Savage, D.E., Curtis, G.H., and James, G.T., 1964, Potassium-argon dates and the Cenozoic mammalian chronology of North America: American Journal of Science, v. 262, p. 145–198.

Farmer, G.L., Glazner, A.F., Wilshire, H.G., Wooden, J.L., Pickthorn, W.J., and Katz, M., 1995, Origin of late Cenozoic basalts at the Cima volcanic field: Journal of Geophysical Research, v. 100, p. 8399–8415.

Faulds, J.E., Feuerbach, D.L., Reagan, M.K., Metcalf, R.V., Gans, P., and Walker, J.D., 1995, The Mount Perkins block, northwestern Arizona: An exposed cross section of an evolving preextensional to synextensional magmatic system: Journal of Geophysical Research, v. 100, p. 15,249–15,266, doi: 10.1029/95JB01375.

Fletcher, J.M., Bartley, J.M., Martin, M.W., Glazner, A.F., and Walker, J.D., 1995, Large-magnitude continental extension: An example from the Central Mojave metamorphic core complex: Geological Society of America Bulletin, v. 107, p. 1468–1483, doi: 10.1130/0016-7606(1995)1072.3.CO;2.

Fliedner, M.M., Klemperer, S.L., and Christensen, N.I., 2000, Three-dimensional seismic model of the Sierra Nevada arc, California, and its implications for crustal and upper mantle composition: Journal of Geophysical Research, v. 105, p. 10,899–10,921, doi: 10.1029/2000JB900029.

Fournier, R.O., 1991, The transition from hydrostatic to greater than hydrostatic fluid pressure in presently active continental hydrothermal systems in crystalline rocks: Geophysical Research Letters, v. 18, p. 955–958.

Fournier, R.O., 1999, Hydrothermal processes related to movement of fluid from plastic into brittle rock in the magmatic-epithermal environment: Economic Geology and the Bulletin of the Society of Economic Geologists, v. 94, p. 1193–1212.

Franceschini, F., 1995, The Larderello plutono-metamorphic core complex: Petrographic data: Proceedings of the World Geothermal Congress, v. 2, p. 667–672.

Gans, P.B., Miller, E.L., McCarthy, J., and Ouldcott, M.L., 1985, Tertiary extensional faulting and evolving ductile-brittle transition zones in the northern Snake Range and vicinity: New insights from seismic data: Geology, v. 13, p. 189–193, doi: 10.1130/0091-7613(1985)132.0.CO;2.

Giggenbach, W.F., 1986, The use of gas chemistry in delineating the origin of fluid discharges over the Taupo volcanic zone: A review: Proceedings of the International Volcanological Congress, New Zealand, v. 5, p. 47–50.

Giggenbach, W.F., 1992, The composition of gases in geothermal and volcanic systems as a function of tectonic setting, in Kharaka, Y.K., and Maest, A.S., eds., Water-rock interaction: Rotterdam, Netherlands, Balkema, p. 873–878.

Giggenbach, W.F., Sano, Y., and Wakita, H., 1993, Isotopic composition of helium, CO_2 and CH_4 contents in gases produced along the New Zealand part of a convergent plate boundary: Geochimica et Cosmochimica Acta, v. 57, p. 3427–3455, doi: 10.1016/0016-7037(93)90549-C.

Glazner, A.F., and Ussler, W., III, 1989, Crustal extension, crustal density, and the evolution of Cenozoic magmatism in the Basin and Range of the western United States: Journal of Geophysical Research, v. 94, p. 7952–7960.

Glazner, A.F., Walker, J.D., Bartley, J.M., Coleman, D.S., and Taylor, W.J., 1994, Igneous activity at releasing bends and transfer zones in extensional systems: Implications for site and mode of geothermal activity: Geothermal Resources Council Transactions, v. 18, p. 7–9.

Groves, K., 1996, Geochemical and isotopic analysis of Pleistocene basalts from the southern Coso volcanic field, California [M.S. thesis]: Chapel Hill, University of North Carolina, 84 p.

Henry, D.J., and Dokka, R.K., 1992, Metamorphic evolution of exhumed middle to lower crustal rocks in the Mojave extensional belt, southern California, USA: Journal of Metamorphic Geology, v. 10, p. 347–364.

Hill, E.J., Baldwin, S.L., and Lister, G.S., 1995, Magmatism as an essential driving force for formation of active metamorphic core complexes in eastern Papua New Guinea: Journal of Geophysical Research, v. 100, p. 10,441–10,451, doi: 10.1029/94JB03329.

Hodges, K.V., McKenna, L.W., Stock, J., Knapp, J., Page, L., Sternlog, K., Silverberg, D., Wust, G., and Walker, J.D., 1989, Evolution of extensional basins and Basin and Range topography west of Death Valley, California: Tectonics, v. 8, p. 453–467.

Holm, D.K., Geissman, J.W., and Wernicke, B., 1993, Tilt and rotation of the footwall of a major normal fault system: Paleomagnetism of the Black Mountains, Death Valley extended terrane, California: Geological Society of America Bulletin, v. 105, p. 1373–1387, doi: 10.1130/0016-7606(1993)1052.3.CO;2.

Huang, W., Silver, L.T., and Kanamori, H., 1996, Evidence for possible horizontal faulting in southern California from earthquake mechanisms: Geology, v. 24, p. 123–126, doi: 10.1130/0091-7613(1996)0242.3.CO;2.

Jackson, J.A., 1987, Active normal faulting and crustal extension, in Coward, M.P., et al., eds., Continental extensional tectonics: Geological Society [London] Special Publication 28, p. 3–17.

Jackson, J., and White, N., 1989, Normal faulting in the upper continental crust: Observations from regions of active extension: Journal of Structural Geology, v. 11, p. 15–36, doi: 10.1016/0191-8141(89)90033-3.

Jones, C.H., Kanamori, H., and Roecker, S.W., 1994, Missing roots and mantle "drips": Regional P_n and teleseismic arrival times in the southern Sierra Nevada and vicinity, California: Journal of Geophysical Research, v. 99, p. 4567–4601, doi: 10.1029/93JB01232.

Jones, C.H., Farmer, L.G., and Unruh, J., 2004, Tectonics of Pliocene removal of lithosphere of the Sierra Nevada, California: Geological Society of America Bulletin, v. 117, no. 11/12, p. 1408–1422.

Lister, G.S., and Baldwin, S.L., 1993, Plutonism and the origin of metamorphic core complexes: Geology, v. 21, p. 607–610, doi: 10.1130/0091-7613(1993)0212.3.CO;2.

Lister, G.S., Banga, G., and Feenstra, A., 1984, Metamorphic core complexes of Cordilleran type in the Cyclades, Aegean Sea, Greece: Geology, v. 12, p. 221–225, doi: 10.1130/0091-7613(1984)122.0.CO;2.

Livaccari, R.F., Geissman, J.W., and Reynolds, S.J., 1995, Large-magnitude extensional deformation in the South Mountains metamorphic core complex, Arizona: Evaluation with paleomagnetism: Geological Society of America Bulletin, v. 107, p. 877–894, doi: 10.1130/0016-7606(1995)1072.3.CO;2.

Manley, C.R., and Bacon, C.R., 2000, Rhyolite thermobarometry and the shallowing of the magma reservoir, Coso volcanic field, California: Journal of Petrology, v. 41, p. 149–174, doi: 10.1093/petrology/41.1.149.

Martinez, F., Taylor, B., and Goodliffe, A.M., 1999, Contrasting styles of seafloor spreading in the Woodlark Basin: Indications of rift-induced secondary mantle convection: Journal of Geophysical Research, v. 104, p. 12,909–12,926, doi: 10.1029/1999JB900068.

Marty, B., and Jambon, A., 1987, $C/^3He$ in volatile fluxes from the solid earth: Implications for carbon geodynamics: Earth and Planetary Science Letters, v. 83, p. 16–26, doi: 10.1016/0012-821X(87)90047-1.

McClusky, S.C., Bjornstad, S.C., Hager, B.H., King, R.W., Meade, B.J., Miller, M.M., Monastero, F.C., and Souter, B.J., 2001, Present day kinematics of the eastern California shear zone from a geodetically constrained block model: Geophysical Research Letters, v. 28, p. 3369–3372, doi: 10.1029/2001GL013091.

Metcalf, R.V., Smith, E.I., Walker, J.D., Reed, R.C., and Gonzales, D.A., 1995, Isotopic disequilibrium among commingled hybrid magmas: Evidence of a two-stage magma mixing-commingling process in the Mt. Perkins pluton, Arizona: Journal of Geology, v. 103, p. 509–527.

Miller, J.S., 1999, Recent perspectives on the dynamics of small-volume rhyolite magma systems from Coso volcanic field, CA: Eos (Transactions, American Geophysical Union), v. 80, p. F1178.

Miller, J.S., and Miller, C.F., 1991, Tertiary extension-related volcanism, Old Woman Mountains area eastern Mojave Desert, California: Journal of Geophysical Research, v. 96, p. 13,629–13,643.

Miller, J.S., Groves, K.R., and Whitmarsh, R.S., 1996, Sources of the Pleistocene Coso rhyolites: A Nd isotopic perspective: Eos (Transactions, American Geophysical Union), v. 77, p. F791.

Misch, P., 1960, Regional structural reconnaissance in central-northeast Nevada and some adjacent areas: Observations and interpretation: Intermountain Association of Petroleum Geologists, 11th Annual Field Conference Guidebook, p. 17–42.

Monastero, F.C., and Unruh, J.R., 2002, Definition of the brittle-ductile transition in the Coso geothermal field, east-central California, USA: Florence, Italy, European Association of Geoscientists and Engineers, Annual Meeting, extended abstracts, May 27–30, 2002.

Monastero, F.C., Katzenstein, A.M., Walker, J.D., and Sabin, A.E., 2002, Neogene evolution of the Indian Wells Valley, east-central California, in, Glazner, A.F., Walker, J.D., and Bartley, J.M., eds., Geologic evolution of the Mojave Desert and southwestern Basin and Range: Geological Society of America Memoir 195, p. 199–228, 3 plates.

Mori, J., and Hartzell, S.H., 1990, Source inversion of the 1998 Upland, California, earthquake: Determination of a fault plane for a small event: Seismological Society of America Bulletin, v. 80, p. 507–518.

Ofoegbu, G.I., and Ferrill, D.A., 1998, Mechanical analyses of listric normal faulting with emphasis on seismicity assessment: Tectonophysics, v. 284, p. 65–77, doi: 10.1016/S0040-1951(97)00168-6.

Oldow, J.S., 2003, Active transtensional boundary zone between the western Great Basin and Sierra Nevada block, western U.S. Cordillera: Geology, v. 31, p. 1033–1036, doi: 10.1130/G19838.1.

Ormerod, D.S., Hawkesworth, C.J., Rogers, N.W., Leeman, W.P., and Menzies, M.A., 1988, Tectonic and magmatic transitions in the western Great Basin: Nature, v. 333, p. 349–353, doi: 10.1038/333349a0.

Pakiser, L.C., Kane, M.F., and Jackson, W.H., 1964, Structural geology and volcanism of Owens Valley region, California—A geophysical study: U.S. Geological Survey Professional Paper 438, 68 p., 2 plates.

Parsons, T., and Thompson, G.A., 1993, Does magmatism influence low-angle normal faulting?: Geology, v. 21, p. 247–250, doi: 10.1130/0091-7613(1993)0212.3.CO;2.

Rahe, B., Ferrill, D.A., and Morris, A.P., 1998, Physical analog modeling of pull-apart basin evolution: Tectonophysics, v. 285, p. 21–40, doi: 10.1016/S0040-1951(97)00193-5.

Rietbrock, A., Tiberi, C., Scherbaum, F., and Lyon-Caen, H., 1996, Seismic slip on a low-angle normal fault in the Gulf of Corinth: Evidence from high-resolution cluster analysis of microearthquakes: Geophysical Research Letters, v. 23, p. 1817–1820, doi: 10.1029/96GL01257.

Roquemore, G.R., 1981, Active faults and associated tectonic stress in the Coso Range, California: Naval Weapons Center Technical Publication TP6270, 101 p.

Schultz, J.R., 1937, A late Cenozoic vertebrate fauna from the Coso Mountains, Inyo County, California: Carnegie Institute of Washington Publication 487, p. 75–109.

Schweig, E.S., III, 1989, Basin-range tectonics in the Darwin Plateau, southwestern Great Basin, California: Geological Society of America Bulletin, v. 101, p. 652–662, doi: 10.1130/0016-7606(1989)1012.3.CO;2.

Serpa, L., and Pavlis, T.L., 1996, Three-dimensional model of the late Cenozoic history of the Death Valley region, southeastern California: Tectonics, v. 15, p. 1113–1128, doi: 10.1029/96TC01633.

Sims, D., Ferrill, D.A., and Stamatakos, J.A., 1999, Role of a ductile décollement in the development of pull-apart basins: Experimental results and natural examples: Journal of Structural Geology, v. 21, p. 533–554, doi: 10.1016/S0191-8141(99)00010-3.

Smith, E.I., Feuerbach, D.L., Naumann, T.R., and Mills, J.G., 1990, Mid-Miocene volcanic and plutonic rocks in the Lake Mead area of Nevada and Arizona: Geological Society of America Memoir 174, p. 169–194.

Stinson, M.C., 1977, Geology of the Keeler 15′ Quadrangle, Inyo County, California: California Division of Mines and Geology, Map Sheet 38, scale 1:62,500.

Stockli, D.F., Surpless, B.E., and Dumitru, T.A., 2000, Late Miocene transition from east-west extension to right-lateral transtension in the central Walker Lane belt: Geological Society of America Abstracts with Programs, v. 32, no. 7, p. 105.

Streitz, R., and Stinson, M.C., 1977, Geologic map of California: Sacramento, California, Death Valley sheet: California Division of Mines and Geology, scale, 1:250,000.

Telford, W.M., Geldart, L.P., Sheriff, R.E., and Keys, D.A., 1976, Applied geophysics: Cambridge, UK, Cambridge University Press, 860 p.

Trexler, J.H., Jr., Cashman, P.H., Henry, C.D., Muntean, T., Schwartz, K., Ten Brink, A., Faults, J.E., Perkins, M., and Kelly, T., 2000, Neogene basins in western Nevada document the tectonic history of the Sierra Nevada–Basin and Range transition zone for the last 12 Ma, in Lageson, D.R., Peters, S.G., and Lahren, M.M., eds., Great Basin and Sierra Nevada: Boulder, Colo-

rado, Geological Society of America Field Guide 2, p. 97–116.

Unruh, J.R., and Streig, A.R., 2004, Mapping and characterization of neotectonic structures in a releasing stepover, northern Coso Range, eastern California: Final technical report submitted to the U.S. Navy Geothermal Program Office, China Lake Naval Air Warfare Center, Contract N68936-02-C-0208, 46 p.

Unruh, J.R., Hauksson, E., Monastero, F.C., Twiss, R.J., and Lewis, J.C., 2002a, Seismotectonics of the Coso Range–Indian Wells Valley region, California: Transtensional deformation along the southeastern margin of the Sierran microplate, in Glazner, A.F., Walker J.D., and Bartley, J.M., eds., Geologic evolution of the Mojave Desert and southwestern Basin and Range: Geological Society of America Memoir 195, p. 277–294.

Unruh, J.R., Monastero, F.C., Pullammanappallil, S., and Honjas, W., 2002b, Upper crustal faulting in an obliquely extending orogen: Structural control on permeability and production in the Coso geothermal field, eastern California: Reno, Nevada, Geothermal Resources Council Proceedings of the Annual Meeting, p. 449–454.

Vittori, E., Michetti, A.M., Slemmons, D.B., and Carver, G., 1993, Style of recent surface deformation at the south end of the Owens Valley fault zone, eastern California: Geological Society of America Abstracts with Programs, v. 25, no. 5, p. 159.

Walker, J.D., Fletcher, J.M., Fillmore, R.P., Martin, M.W., Taylor, W.J., Glazner, A.F., and Bartley, J.M., 1995, Connection between igneous activity and extension in the central Mojave metamorphic core complex, California: Journal of Geophysical Research, v. 100, p. 10,477–10,494, doi: 10.1029/94JB03132.

Weaver, C.S., and Hill, D.P., 1979, Earthquake swarms and local crustal spreading along major strike-slip faults in California: Pageoph, v. 117, p. 51–64, doi: 10.1007/BF00879733.

Welhan, J.A., Poreda, R.J., Rison, W., and Craig, H., 1988, Helium isotopes in geothermal and volcanic gases of the western United States, I., Regional variability and magmatic origin: Journal of Volcanology and Geothermal Research, v. 34, p. 185–189, doi: 10.1016/0377-0273(88)90032-7.

Wernicke, B.P., 1981, Low-angle normal faults in the Basin and Range Province: Nappe tectonics in an extending orogen: Nature, v. 291, p. 645–648, doi: 10.1038/291645a0.

Wernicke, B.P., 1992, Cenozoic extensional tectonics of the U.S. Cordillera, in, Burchfiel, B.C., et al., eds., The Cordilleran orogen: Conterminous U.S.: Boulder, Colorado, Geological Society of America, Geology of North America, v. G-3, p. 553–581.

Wernicke, B.P., 1995, Low-angle normal faults and seismicity: A review: Journal of Geophysical Research, v. 100, p. 20,159–20,174, doi: 10.1029/95JB01911.

Wernicke, B.P., and Axen, G.J., 1988, On the role of isostasy in the evolution of normal fault systems: Geology, v. 16, p. 848–851, doi: 10.1130/0091-7613(1988)0162.3.CO;2.

Wernicke, B.P., Spencer, J.E., Burchfiel, B.C., and Guth, P.L., 1982, Magnitude of crustal extension in the southern Great Basin: Geology, v. 10, p. 489–502.

White, W.M., Hofmann, A.W., and Pachett, H., 1987, Isotope geochemistry of Pacific mid-ocean ridge basalts: Journal of Geophysical Research, v. 92, p. 4881–4893.

Whitmarsh, R.S., 1998, Geologic map of the Coso Range: Geological Society of America on-line map, doi: 10.1130/1998-whitemarsh-coso.

Wilson, C.K., Jones, C.H., and Gilbert, H.J., 2003, A single-chamber silicic magma system inferred from shear-wave discontinuities of the upper crust and uppermost mantle, Coso geothermal area, California: Journal of Geophysical Research, v. 108, 226, doi: 10.1029/2002JB001798.

Wust, S.L., 1986, Regional correlation of extension directions in cordilleran metamorphic core complexes: Geology, v. 14, p. 828–830, doi: 10.1130/0091-7613(1986)142.0.CO;2.